

SSC-194

FEASIBILITY STUDY OF MODEL TESTS ON SHIP HULL GIRDERS

This document has been approved
for public release and sale; its
distribution is unlimited.

SHIP STRUCTURE COMMITTEE

MAY 1969

SHIP STRUCTURE COMMITTEE

MEMBER AGENCIES:

UNITED STATES COAST GUARD
NAVAL SHIP SYSTEMS COMMAND
MILITARY SEA TRANSPORTATION SERVICE
MARITIME ADMINISTRATION
AMERICAN BUREAU OF SHIPPING

ADDRESS CORRESPONDENCE TO:

SECRETARY
SHIP STRUCTURE COMMITTEE
U.S. COAST GUARD HEADQUARTERS
WASHINGTON, D.C. 20591

May 1969

Dear Sir:

The strength of structural elements such as flat plates, stiffened plates and grillages, has received considerable attention in order to arrive at some rational methods of ship structural design. However, to effectively utilize the elemental results, it becomes increasingly important to determine the interaction between the separate elements and hence, the ultimate strength of a hull girder.

Herewith is a report entitled *Feasibility Study of Model Tests on Ship Hull Girders* by Herbert Becker that is a result of a project sponsored by the Ship Structure Committee.

This report is being distributed to individuals and groups associated with or interested in the work of the Ship Structure Committee. Comments concerning this report are solicited.

Sincerely,



D. B. Henderson
Rear Admiral, U. S. Coast Guard
Chairman, Ship Structure Committee

SSC-194

Final Report

on

Project SR-183

"Large-Scale Design Testing"

to the

SHIP STRUCTURE COMMITTEE

FEASIBILITY STUDY OF MODEL TESTS ON SHIP HULL GIRDERS

by

Herbert Becker

MITHRAS

Cambridge, Massachusetts

under

Department of the Navy
Naval Ship Engineering Center
Contract N00024-68-C-5468

This document has been approved
for public release and sale; its
distribution is unlimited.

U. S. Coast Guard Headquarters
Washington, D. C.

May 1969

ABSTRACT

An efficient program is identified for ultimate strength testing of hull girder models representative of longitudinally framed ship construction. The purpose of the tests is to generate data (for correlation with theory where available) to provide the basis for engineering design of the primary structure of the hull girder. The major loads are longitudinal compression induced by primary hull bending, normal pressure from the sea, and athwartship compression induced by the horizontal pressure on the sidewalls.

This report discusses loadings, strength theory and available experimental data, and experimental mechanics techniques, to develop rationally the general character of a testing project which could provide satisfactory data for correlation with theory at low cost in a moderate period of time.

The results of the evaluation indicate the feasibility of a project which would begin with a number of compression tests using steel box models less than one foot long. The purpose is to establish basic behavior and to provide inputs to assist in developing a reliable strength theory which would have general utility over a wide range of parameters relevant to hull girder design.

CONTENTS

	<u>Page</u>
SYMBOLS	v
NOMENCLATURE	vii
INTRODUCTION	1
LOADINGS	4
STRENGTH THEORIES AND EXPERIMENTAL DATA	6
EXPERIMENTAL MECHANICS	24
OPTIMUM EXPERIMENTAL PROGRAM	26
MATERIAL SELECTION	26
MODEL FABRICATION	27
MODEL DESIGN	29
MODEL LOADING SYSTEMS	34
CONCLUSIONS	35
RECOMENDATIONS	36
ACKNOWLEDGMENTS	40
REFERENCES	40
APPENDIX I - ULTIMATE STRENGTH OF PLATES	43
APPENDIX II - SHELL THEORY FOR PLATE BUCKLING UNDER PRESSURE	45
APPENDIX III - BIAXIAL BUCKLING OF FLAT PLATES	47
APPENDIX IV - NONDESTRUCTIVE TESTING FOR STRUCTURAL STABILITY	48

SHIP STRUCTURE COMMITTEE

The SHIP STRUCTURE COMMITTEE is constituted to prosecute a research program to improve the hull structures of ships by an extension of knowledge pertaining to design, materials and methods of fabrication.

RADM D. B. Henderson, USCG - Chairman
Chief, Office of Engineering
U. S. Coast Guard Headquarters

Captain William R. Riblett
Head, Ship Engineering Division
Naval Ship Engineering Center

Mr. E. Scott Dillon
Chief, Division of Ship Design
Office of Ship Construction
Maritime Administration

Captain T. J. Banvard, USN
Maintenance and Repair Officer
Military Sea Transportation Service

Mr. D. B. Bannerman, Jr.
Vice President - Technical
American Bureau of Shipping

SHIP STRUCTURE COMMITTEE

The SHIP STRUCTURE SUBCOMMITTEE acts for the Ship Structure Committee on technical matters by providing technical coordination for the determination of goals and objectives of the program, and by evaluating and interpreting the results in terms of ship structural design, construction and operation.

NAVAL SHIP ENGINEERING CENTER

Mr. J. J. Nachtsheim - Chairman
Mr. J. B. O'Brien - Contract Administrator
Mr. George Sorkin - member
Mr. H. S. Sayre - Alternate
Mr. Ivo Fioriti - Alternate

MARITIME ADMINISTRATION

Mr. Frank Dashnaw - Member
Mr. Anatole Maillar - Member
Mr. R. Falls - Alternate
Mr. W. G. Frederick - Alternate

AMERICAN BUREAU OF SHIPPING

Mr. G. F. Casey - Member
Mr. F. J. Crum - Member

OFFICE OF NAVAL RESEARCH

Mr. J. M. Crowley - Member
Dr. Wm. G. Rauch - Alternate

MILITARY SEA TRANSPORTATION SERVICE

LCDR R. T. Clark, USN - Member
Mr. R. R. Askren - Member

U. S. COAST GUARD

CDR C. R. Thompson, USCG - Member
CDR J. L. Howard, USCG - Member
LCDR Leroy C. Melberg, USCG - Alternate
LCDR R. L. Brown, USCG - Alternate

NAVAL SHIP RESEARCH & DEVELOPMENT CENTER

Mr. A. B. Stavovy - Alternate

LIAISON REPRESENTATIVES

NATIONAL ACADEMY OF SCIENCES-
NATIONAL RESEARCH COUNCIL

Mr. A. R. Lytle - Technical Director, Maritime
Transportation Research Board

Mr. R. W. Rumke - Executive Secretary, SRC

AMERICAN IRON AND STEEL INSTITUTE

Mr. J. R. Lecron

BRITISH NAVY STAFF

Mr. H. E. Hogben
Staff Constructor Officer
Douglas Faulkner, RCNC

WELDING RESEARCH COUNCIL

Mr. K. H. Koopman, Director
Mr. Charles Larson, Secretary

SYMBOLS

A	bulkhead spacing (in.)
A_s	area of stiffener, in. ²
\bar{A}	area, in. ²
a	length of plate (same as spacing of transverse frames), in.
B	width of ship beam, in.
b	width of plate (same as spacing of longitudinals), in.
b_e	effective width of buckled plate, in.
C	coefficient for cylinder buckling, a function of r/t (see Figure A2)
c	distance from neutral axis to extreme fiber of beam, in.
D	stiffness of plate in bending, $Et^3/[12(1-\nu_e^2)]$, in-lb.
d	stiffener depth, in.
E	Young's modulus, Msi (1 Msi = 10 ⁶ psi)
E_s	secant modulus on stress-strain curve ($= \sigma/\epsilon$), Msi
E_t	tangent modulus on stress-strain curve ($= d\sigma/d\epsilon$), Msi
F	parameter, $(t/b)(E/\sigma_{cy})^{1/2}$
f	factor of safety
H	depth of hull girder, in.
I	moment of inertia of cross section, in ⁴ .
k	buckling coefficient
L	length, in. (ship; also, beam-column (Appendix IV))
M	bending moment, in-lb.
m	number of longitudinal half waves in buckled plate
N	loading, force per unit distance along section normal to load, lb/in.
n	exponent in theoretical strength relation
P	axial force on column, lb.
p	pressure, psi
Q	transverse concentrated load on beam, lb.
R	stress ratio, Eqs. (18), (19)
r	radius of cylinder (in.)
S	parameter used in design of stiffened plating (pd/t), psi
s	number of transverse half waves in buckled plate
t	plate thickness, in.

\bar{t}	effective thickness of plate plus longitudinal stiffener ($t + A_s/b$), in.
U	unevenness factor (Figure A2)
w	lateral deflection
w_o	initial lateral deflection or initial imperfection
a	parameter, $(p/E)(b/t)^4$
δ	lateral motion induced by Q (Appendix IV)
ϵ	strain
η	plasticity reduction factor for inelastic buckling, Eqs. (3), (4)
ν	Poisson's ratio
ν_e	elastic Poisson's ratio
ν_p	fully plastic Poisson's ratio (usually 1/2)
ρ	radius of gyration of cross section, in.
Σ	scale factor
σ	stress, ksi
σ_o	reference stress for buckling, $\pi^2 D/b^2 t$, ksi
\$	cost, dollars

Subscripts

a	allowable
col	column buckling
cr	critical (or buckling)
cy	compressive yield
f	flange of longitudinal stiffener
m	model
p	prototype also, pressure
pl	plate
r	residual
u	ultimate
w	web of longitudinal stiffener
x	longitudinal
y	athwartship, or transverse
z	vertical

NOMENCLATURE

The structural components of a representative region of a longitudinally framed hull bottom appear in outline form in Figure 1, which delineates the terminology used throughout this report. The related boundary requirements for buckling and failure are also identified in Figure 1. These terms are defined as follows:

instability	the limit of structural load carrying capacity determined by a change in structural state
buckling	change in structural state from flat to bent (or lobar) form
critical	synonymous with buckling (buckling stress = σ_{cr})
column buckling	buckling of the longitudinal stiffeners between transverse frames
plate buckling	lobar form within $x = 0, a$ and $y = 0, b$. Equal to, or less than, failure
panel buckling	lobar form within $x = 0, a$ and $y = 0, B$. Equivalent to column buckling. Also equivalent to failure. May include the plate buckle mode as well as the column mode.
grillage buckling	lobar form within $x = 0, A$ and $y = 0, B$. Equivalent to total collapse. May include both plate and column modes as well as grillage mode.
instability failure	complete loss of ability to carry load
postbuckling regime	symbolically, $\sigma_{cr} \leq \sigma \leq \sigma_u$

These terms are discussed more fully in the section on strength theories.

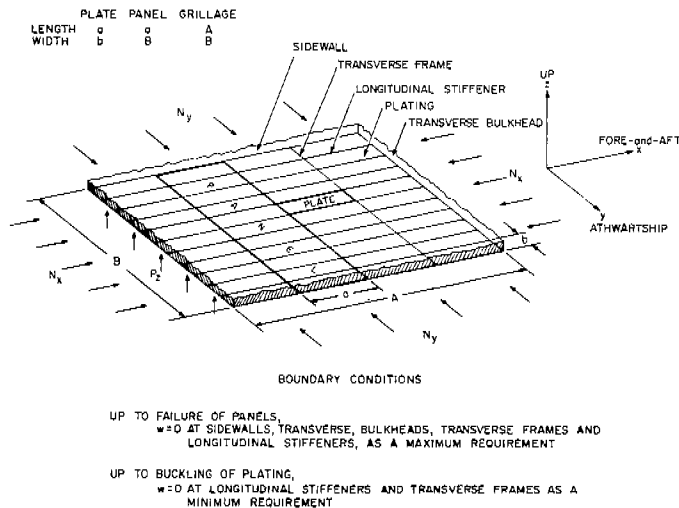


Fig. 1 Schematic Layout of a Typical Structural Grillage.

INTRODUCTION

Purpose of Proposed Program

Hull girder model studies for ultimate strength determination can provide large quantities of reliable experimental data at reasonable cost and in a reasonable period of time provided that a careful planning of the test program precedes the fabrication and the testing of the models. It is the purpose of this investigation to discuss the background of data utilized to evaluate the factors which would influence the design and test of a scale model of a longitudinally framed hull girder box beam, to present the conclusions of those investigations, and to arrive at recommendations for an efficient test program through rational application of the results and conclusions of this investigation.

The prime focus of the investigation was upon the definition and identification of the important parameters affecting the design and test of the model. No consideration was given to the availability of existing facilities. This was done in order to remove any bias on that factor which might conceivably militate against achieving the most effective type of experimental program. It was considered likely, however, that any of a relatively large number of existing test facilities would be capable of handling the end product of this investigation.

Numerous factors influence the characteristics of the optimum model. These relate to the types of loads, the nature of failure, methods of measuring strains and deformations, various procedures for applying load, and (most important of all) the state of the art in regard to theoretical procedures for predicting collapse. They are discussed in this report in sufficient detail to provide the basis for arriving at the conclusions and recommendations at the end.

Major Problem

At the present time, surface vessels for the Navy are designed on the basis of Design Data Sheet No. 1100-3. Basically, it contains curves on the cross section of a relatively long compressed flat plate (loading = N_x) with simply supported edges. These are identified schematically in Figure 2. The data were obtained from panel tests with simple support structural configurations.

The actual behavior of a bottom structure involves not only longitudinal compression of a series of longitudinally stiffened plates, but also includes the effect of lateral pressure, p_z , and the effect of transverse membrane loadings, N_y , from the forces acting on the sides of the vessel. This combined condition may have an influence upon the nature of the curves shown in Figure 2.

It is the fundamental mission of this investigation to develop ground rules for the fabrication of models to test, reliably and to a high degree of accuracy, such variations of Figure 2 as may be induced by N_y and p_z . The principal focus of new theoretical methods of analysis should be upon these aspects of the problem. Current theories are discussed in this report. Furthermore, the present state of test data on these problem areas is considered carefully and evaluated in the light of existing theory.

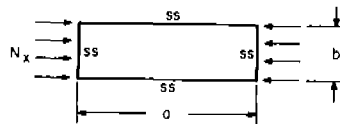
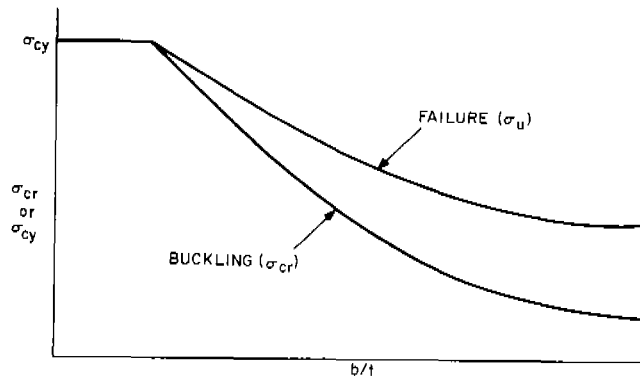


Fig. 2 Basic Design Chart.

Other Problem Areas

The scope of the current study has been limited to combinations of longitudinal compression, transverse compression and normal pressure on a structural grillage representative of a hull bottom. Other problem areas could arise from torsion loads and vertical shear on ships with large openings, which include both tankers and container ships. On deep vessels the combination of these latter loadings with transverse compression and normal pressure could induce buckling, and possibly failure.

Shear load problem areas have not been included in the listing of experiments recommended for the initial effort to evaluate hull girder strength. They are listed among the topics suggested for follow-on after the initial phase is completed.

Basic Approach

This investigation is a feasibility study. The project is aimed at identifying the parameters which should be considered in designing and conducting tests on small, medium and large scale models. Specific details are presented for models which appear to offer most effectively the range of data necessary to establish a sound basis for design.

In addition to the experimental aspects of the project, considerable emphasis is placed upon the need for a theoretical approach at the time that required testing may actually be performed. This report includes discussion of the possibilities of developing theories which do not exist at present, and careful evaluations of current theories. However, a detailed evaluation of all theories is not presented. Rather, that task is left for the experimental/theoretical investigation to follow this project.

Reference Ship

Many of the discussions in this report pertain to general aspects of hull girder strength. In order to provide a basis for specific details of geometry and loading, some of the design information for a fast combat support ship, AOE 2, have been utilized. These include the basic dimensions, bending moment diagram and stresses. That information is not repeated in this report. It was only used as a guide throughout this project.

Model Size

The factor of model size influences every aspect of this investigation, as it would do in the case of an actual experimental/theoretical project. It influences the selection of strain gages on models which may be small and therefore may have relatively thin walls, and the selection of strain gages for very large scale models because of the number which may be required in order to cover reliably a sufficient area of the model to provide coverage of data. Naturally, it would have a major influence in areas in which unfairness of plating is a factor since it may be difficult to scale unfairness throughout a large range of model sizes. Model sizes would have a pronounced influence on cost and testing time.

Materials Selection

The character of Figure 2 was obtained from data on current naval steels. The present trend in ship construction is towards the use of steels with yield strengths approaching 100 ksi. Since the buckling stress is unaffected by the yield strength level until the proportional limit of the material is reached, then there would be an immediate influence felt on the relationship between effective stress and b/t . The elastic range would continue to much lower b/t than at present. These factors are taken into consideration in the discussions which are included on materials selection. Furthermore, the nature of the stress-strain curve in the region of the proportional limit and yield could have an influence upon the relationship between σ_{cr} and σ_u .

Optimum Testing

The culmination of the evaluations presented in this report is the section on optimum testing. The parameters which affect model size, types of experimental mechanics procedures, and numbers and types of tests are considered with regard to the technical aspects of the program as well as to cost and time for the project. The optimization proceeds with consideration of these factors. The optimum costs test would, naturally, involve nothing but very small models which would be few in number. The same would be true for a minimum time investigation. However, it is not necessarily true that these investigations would provide sufficient reliable technical data. Consequently, the test optimization involves the proper balance of cost and time with the acquisition of satisfactory amounts of experimental data for correlation with theory. It is the drawing of that balance which is involved in the section on optimum testing.

Appendices

Several topics of relevance to this investigation are covered in the four appendices. They have been relegated to that section to avoid interrupting the mainstream of the report.

The first three appendices furnish theoretical data. Appendix I presents a theory for predicting the ultimate strength of compressed flat plates. Appendix II presents a recent development in the calculation of plate buckling under axial compression and transverse compression. Appendix III is a recapitulation of biaxial compression buckling theory for flat plates, while Appendix IV describes results of research into the experimental prediction of buckling.

LOADINGS

Introduction

The development of proper experimental models requires a clear understanding of the loadings to be simulated. This section contains a description of the forces exerted on a ship by the sea, a discussion of the manner in which those external forces induce loads on components of the ship, and an evaluation of the influence of construction details on the components (bottom, intermediate decks, sidewalls).

Forces from the Sea

A ship at sea is subjected to pressures, temperatures and inertia forces. The loading condition which corresponds most closely to longitudinal strength design (the subject of interest in this project) would involve pressures only. The other effects need not be considered.

The pressure distribution causes longitudinal, athwartship and vertical forces on the hull exterior. These induce vertical shear, longitudinal bending, athwartship shear, athwartship bending, torsion, athwartship compression, and longitudinal compression. The focus of this investigation is on the combination of longitudinal bending and athwartship compression, together with the local action of bottom pressure. The distributions of those forces are displayed schematically in Figure 3.

Loads on Components

Consider a simple box to represent the hull girder of a ship. The sea forces of interest would induce loads on the deck, bottom and sidewalls.

The loading for which the ship usually would be designed is the longitudinal membrane compression in the bottom due to bending. The effect of bottom normal pressure is frequently taken into account through a simple interaction relation

$$\sigma_x / (f \sigma_{x_{cr}}) + \sigma_p / \sigma_a = 1 \quad (1)$$

However, this does not include the effect of pressure on $\sigma_{x_{cr}}$, nor does it consider the ultimate strength of the bottom. As is evident from Figure 3, this load combination would be greatest during hogging, when

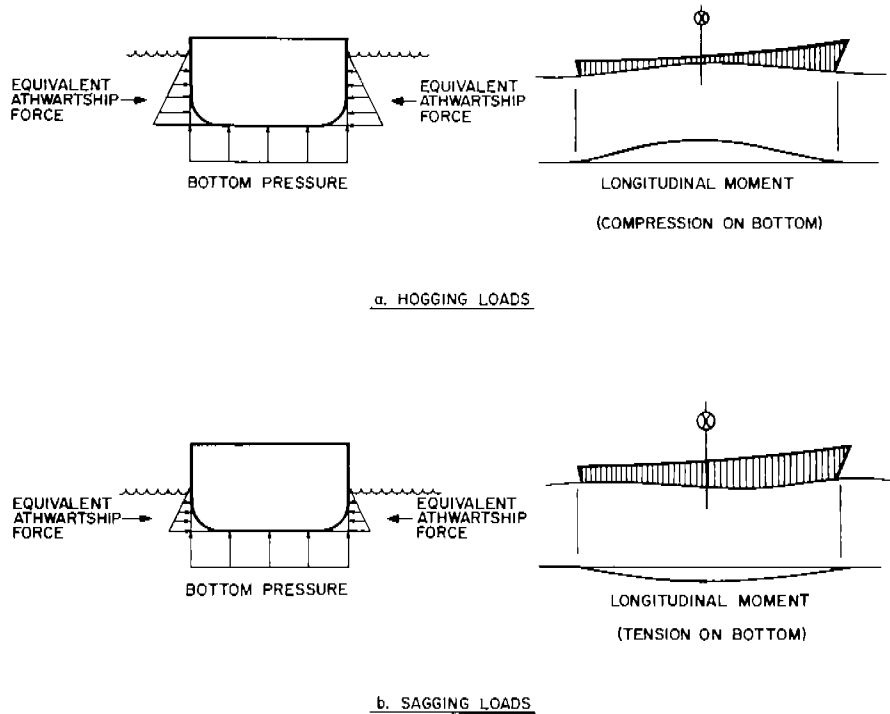


Fig. 3 Representation of Loadings Considered in This Investigation.

the peak bending moment and peak normal pressure would occur simultaneously.

At present the effect of athwartship forces is not considered in design. This could be an unconservative practice for a deep ship, since the athwartship membrane compression on the bottom would tend to reduce the longitudinal compression buckling stress and might also affect σ_u whether or not the bottom normal pressure is considered. For example, if the waterline is 60 ft. above the keel, the bottom pressure would be approximately 25 psi, and the transverse membrane loading would be

$$N_y = (2/3) (25) (60) \times (12) = 12,000 \text{ lb/in}$$

if there were no intermediate decks. This could be a large fraction of N_x .

The possibilities of further complication from lateral bending and shear should be considered also. However these effects could be deferred to a subsequent study. Initially, the major problem is left to involve N_x , N_y and P_z .

Effects of Internal Structure

Insofar as bending is concerned, it is assumed that load diffusion effects are absent and that $\sigma_b = Mz/I$ at all levels in the ship. Therefore, there would be no need to consider internal details such as intermediate decks or longitudinal bulkheads in calculating the longitudinal compression on the stiffened plating in the bottom region of the strength envelope. Furthermore, since the sea acts directly on the bottom, the local pressure loading also would be essentially independent of internal structural details. Ribs and longitudinal bulkheads or deep girders would act to define panel sizes and possibly to provide some measure of end fixity.

The distribution of athwartship membrane forces, on the other hand, would be dependent upon the possible presence of intermediate decks and rigid longitudinals. If the decks extend to the sidewalls, they would resist the lateral pressure directly. If they are completely internal, a load diffusion analysis would be required to determine the magnitude of athwartship forces on the bottom. Consequently, the development of proper modeling of these two different cases would require ingenuity in order to avoid an excessive number of models. Some possibilities are discussed in the Model Design section.

STRENGTH THEORIES AND EXPERIMENTAL DATA

Introduction

Modes of Failure

The problem under examination revolves around the nature of the structural behavior of longitudinally stiffened plating subjected to longitudinal membrane compression forces in the neutral plane of stiffened plating, membrane compression forces acting perpendicular to the longitudinal forces in the plane of the plating midthickness, and normal pressure applied perpendicular to the stiffened plating on the unstiffened face. This system of loads is depicted schematically in Figure 4. The Nomenclature may be consulted for reference to the terms used in this discussion.

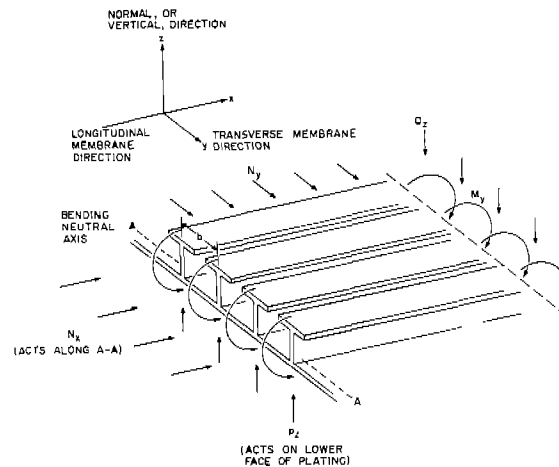


Fig. 4 Load System Acting on Longitudinally Stiffened Section Grillage.

If two y-direction node lines are assumed to be enforced by a pair of transverse frames at a spacing, a , three important types of instability may be identified:

- 1) The plates may buckle between longitudinals and frames, while the longitudinals remain straight.
- 2) The panel of plating plus stiffeners may buckle as a wide column between transverse frames before (or just as) the plate may buckle.
- 3) The plates may buckle, after which the longitudinal stiffener system may support additional load until the columns buckle, at which point the panel will fail.

Through general use, condition 1) is referred to as buckling, whereas conditions 2) and 3) are referred to as failure. The load carrying capacity at collapse is termed strength.

The difference between plate strength and panel strength is a necessary distinction. Plate strength is the average stress level induced by the maximum load acting on a plate (of length a and width b) which is supported along the edges by mechanical devices that carry no load but enforce a straight line along each edge.

A panel buckles and fails basically as a column. Panel strength is the mean stress level at the maximum load on a plate-stiffener system with no edge supports, but with attached longitudinals of length a and spacing b . Panel strength may be less than, equal to, or greater than plate strength since it depends largely upon the character of the longitudinals.

Another type of instability is possible in a longitudinally framed ship if the transverse frames are not sufficiently stiff to enforce a node line across the longitudinals. The transverse frames conceivably could buckle before the longitudinals fail as columns. In that case general instability would occur involving the entire rectangular region of the bottom between the sidewalls and between the bulkheads. This form of instability is not considered in the current problem. In naval architecture the term "general instability" is also applied to the condition which is identified here as panel instability.

General treatment of the field of structural stability may be found in the critical survey by Gerard and Becker (Ref. 1), which contains detailed critical evaluations of theory and experiment. Cooper's bibliography may also be used to locate data more directly pertinent to ship construction (Ref. 2).

Status of Theory and Experiment

There are several aspects to the problem under investigation. The following tabulation outlines the status of theory and experiment in each relevant category. Detailed discussions appear in the following portions of this section. Also consult Table 1.

Table 1. Status of Theory and Experiment on Pertinent Features of Pressurized Stiffened Panel Behavior

Feature			Theory	Experiment
Plating, p = 0	Uniaxial Comp.	σ_{cr}	Extensive	Extensive
		σ_u	Yes	Yes
	Biaxial Comp.	σ_{cr}	Yes	No
		σ_u	No	No
Plate p > 0	Uniaxial Comp.	σ_{cr}	Yes	Yes
		σ_u	No	No
	Biaxial Comp.	σ_{cr}	No	No
		σ_u	No	No
Panel p = 0	Uniaxial Comp.	σ_{cr}	Extensive	Extensive
		σ_u	Yes	Yes
	Biaxial Comp.	σ_{cr}	No	No
		σ_u	No	No
Panel p > 0	Uniaxial Comp.	σ_{cr}	Yes	Yes
		σ_u	Yes	Yes
	Biaxial Comp.	σ_{cr}	No	No
		σ_u	No	No
Grillages	Uniaxial Comp.	σ_{cr}	Yes	Yes
		σ_u	Yes	Yes
	Biaxial Comp.	σ_{cr}	No	No
		σ_u	No	No
Effects of Residual Stress			Yes	Yes
Design Optimization			Yes	Yes

Compression Buckling of Flat Plates

Basic Data for Long Plates

For plates in a longitudinally framed ship, a/b usually is of the order of 3 or 4, in which case, Bryan's theoretical buckling relation

$$\sigma_{cr} = \eta \frac{k\pi^2 E}{12(1 - \nu_e^2)} \left(\frac{t}{b}\right)^2 \quad (2)$$

applies with k = 4 (Ref. 3).

The plasticity reduction factor, η depends upon the stress level and the shape of the stress-strain curve in the yield region. It represents recognition of the fact that buckling can occur inelastically. That is to say, the change from flat to lobar form can occur at a stress level in the yield region of the stress-strain curve. For steels this range is small (Figure 5). For aluminum alloys, however, it can be large, and permanent deformations after load release may be apparent after elastic buckling in aluminum, whereas insignificant residuals may be observed in steel plates which have buckled elastically. Furthermore, buckling stresses may reach the plastic region in aluminum much sooner (as a percentage of σ_{CY}) than in steel. In such a case it is necessary to modify the usual elastic theory of plate buckling to account for this fact. That is done by introduction of η , a term which has been derived from fundamental theoretical considerations by Stowell (Ref. 4) and by Gerard (Ref. 5) for several cases of thick plate buckling. It reduces the hypothetical elastic buckling stress to the actual value on the stress-strain curve, but not necessarily at the same strain as the elastic value.

Mathematically, η is equal to

$$\eta = \frac{1 - \nu^2}{1 - \nu} \frac{e}{2} (E_s/E) \left[(1/2) + (1/4) (1 + 3E_t/E_s)^{1/2} \right] \quad (3)$$

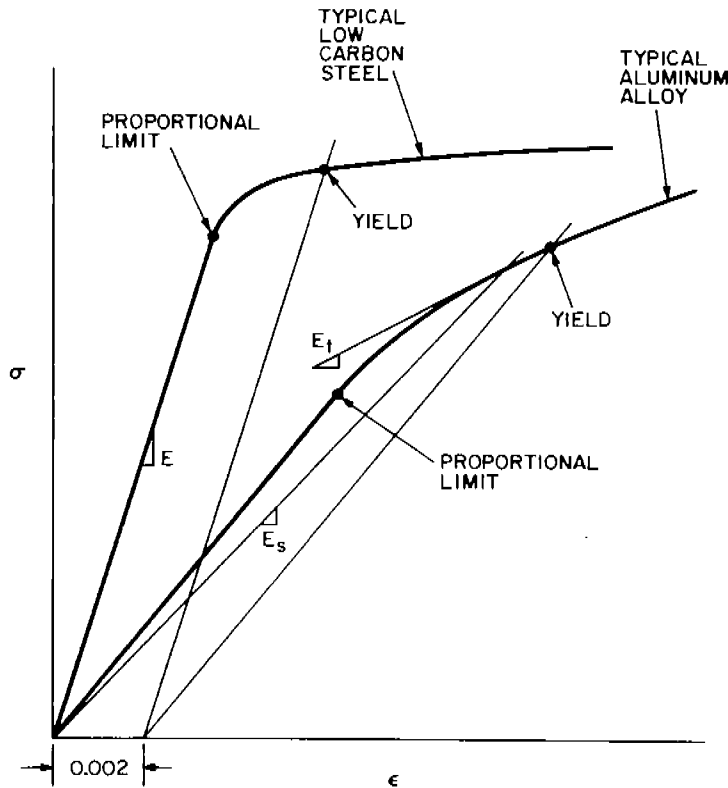


Fig. 5 Stress-Strain Curves for Steel and Aluminum.

for simply supported edges and

$$\eta = \frac{1 - \nu_e^2}{1 - \nu^2} (E_s/E) \left[0.352 + 0.324 (1 + 3E_t/E_s)^{1/2} \right] \quad (4)$$

for clamped edges where the inelastic value of Poisson's ratio, as derived by Gerard and Wildhorn (Ref. 6), is

$$\nu = \nu_p - (\nu_p - \nu_e) (E_s/E) \quad (5)$$

The character of the agreement of theory with experiment for ship plating of various steels was ascertained by Vasta (Ref. 7) and reported in the open literature by Frankland (Ref. 8) as shown in Figure 6. The same agreement is observed for other structural metals, except where σ_{cr} approaches σ_{cy} in which range the shape of the knee of the stress-strain curve exerts an influence, as discussed above.

Theory is seen to agree well with experiment up to the proportional limit, after which the agreement can be maintained if the plasticity reduction factor is taken into account. Such data are not reported in Ref. 7. However, an indication of the agreement can be seen in Figure 7 for flanges, for which the plasticity reduction factor is obtainable from

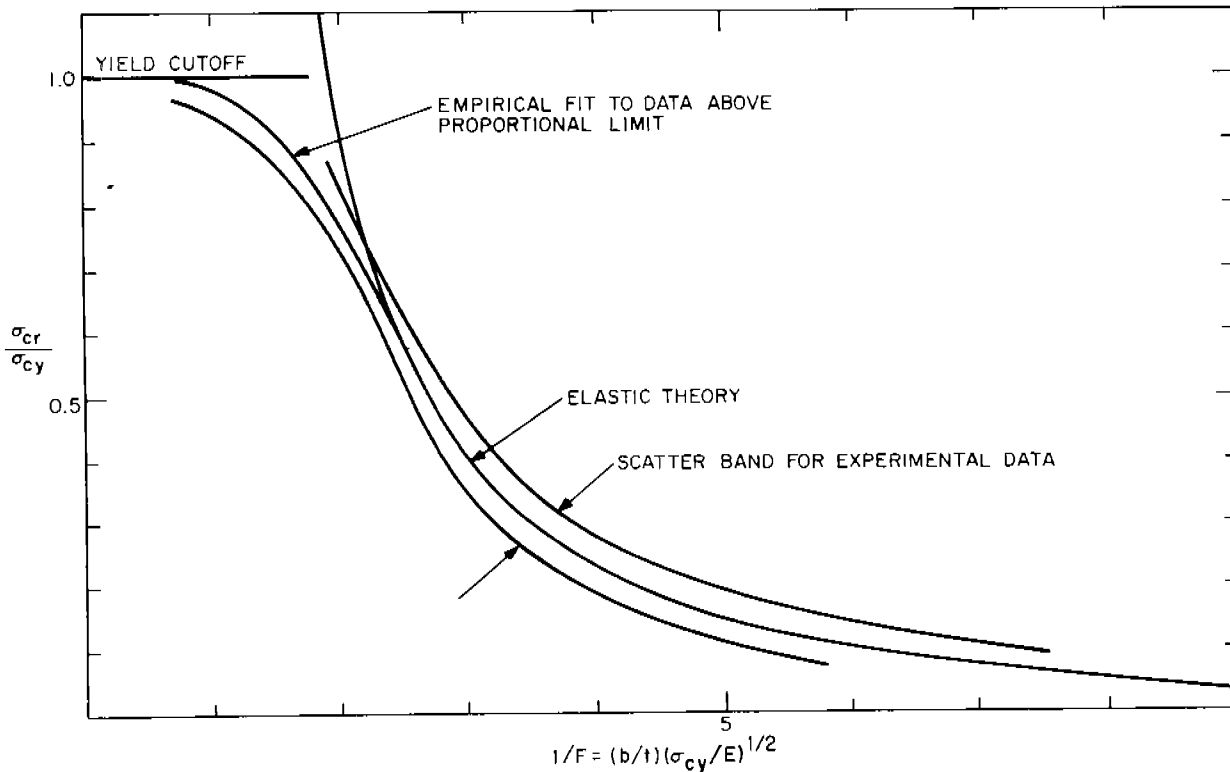


Fig. 6 Typical Buckling Data for Uniaxially Compressed Plates.

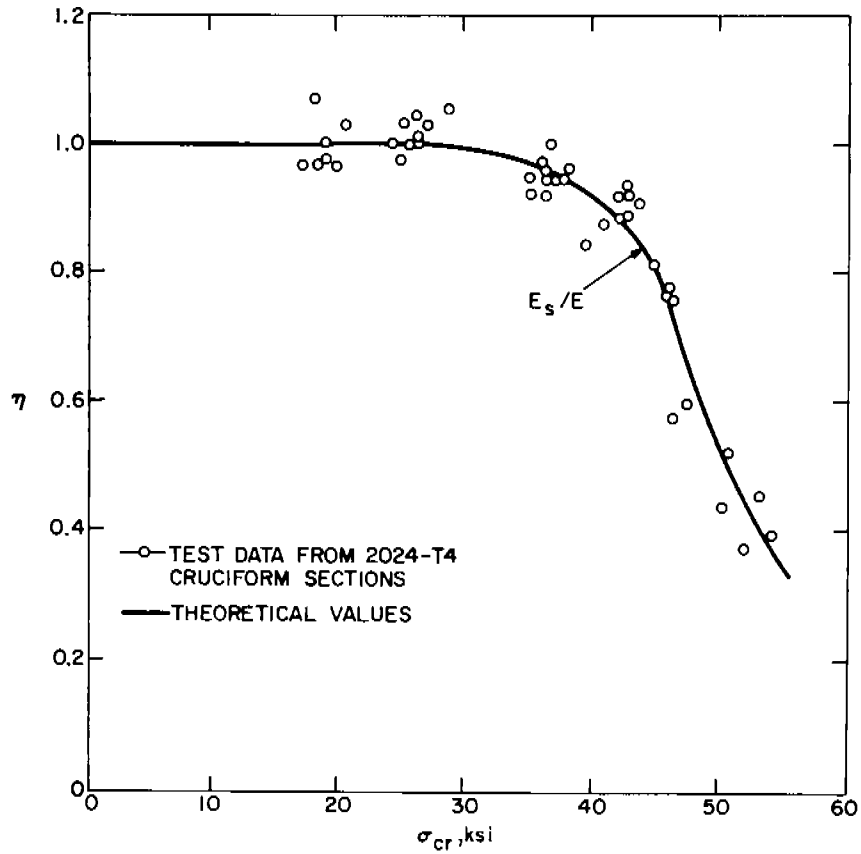


Fig. 7 Comparison of Theory and Experiment for Compressed Simply Supported Flanges (Ref. 1).

$$\eta = \frac{1 - \nu^2}{1 - \nu} \left(\frac{E_s}{E} \right) \quad (6)$$

Effect of Aspect Ratio

In general, the buckling coefficient is

$$k = (a/mb + mb/a)^2 \quad (7)$$

in which m is the number of half-waves in the length a . If the plate buckles in square waves, which would happen if $a/b = 1$, then $k = 4$ as used above.

If $m = 1$ and $a/b < 1$ (which would be the case for a wide plate), then

$$k = (b/a)^2 \left[1 + (a/b)^2 \right] \quad (8)$$

and

$$\sigma_{cr} = \left[1 + (a/b)^2 \right] \frac{\pi^2 E}{12 (1 - \nu_e^2)} \left(\frac{t}{a} \right)^2 \quad (9)$$

The buckling stress for a simply supported plate consists of the expression for the buckling stress of a wide column

$$\sigma_{col} = \frac{\pi^2 E}{12 (1 - \nu_e^2)} \left(\frac{t}{a} \right)^2 \quad (10)$$

modified by the factor $\left[1 + (a/b)^2 \right]$. If a/b is of the order of $1/5$, the error involved in disregarding the factor would be conservative by 4 percent. Consequently, if compression tests are performed on longitudinally stiffened panels with free unloaded edges, the behavior should approximate ship structural behavior since the transverse frame spacing is normally a small fraction of the ship beam width. The only additional factor to be considered is the term $1 - \nu_e^2$, which represents plate behavior. It is absent in the column buckling equation

$$\sigma_{col} = \frac{\pi^2 E \rho^2}{a^2} \quad (11)$$

where

$$\rho^2 = t^2/12.$$

Effect of Residual Stresses

Experiments conducted by Rampetsreiter, Lee and Ostapenko (Ref. 9) show that, when longitudinal stiffeners are welded to a plate, the residual longitudinal compression stress, σ_r , would reduce the buckling stress of a plate in longitudinal compression by σ_r , so that

$$\sigma_{cr} = \sigma_{cr_r} + \sigma_r \quad (12)$$

The scatter in the experimental data is large. As a result the correlation was obtained from averaged values of the residual stress distribution.

The presence of residual stress would tend to reduce the buckling stress of plating between stiffeners, as shown above. However, the stiffeners would be loaded in tension and also would tend to curve somewhat. As a result, if plate buckling and column buckling were to occur simultaneously because the stiffeners were unable to support load after the buckling of the plate, then the panel strength would be reduced. If the stiffeners are sufficiently rigid to carry load beyond buckling, then a reduction in σ_u might be anticipated.

Effect of Initial Imperfections

An important aspect of the stability characteristics of a structure is the influence upon buckling and collapse which can be exerted by departure of the fabricated initial shape from theoretically perfect form. These departures are often referred to as initial imperfections, or unfairness.

On the basis of theoretical considerations and test data, it is now well known that the role of unfairness depends upon the shape of the structure and the type of loading to be applied. Three cases are shown schematically in Figure 8, which depicts the load loss, $\Delta\sigma$, due to the

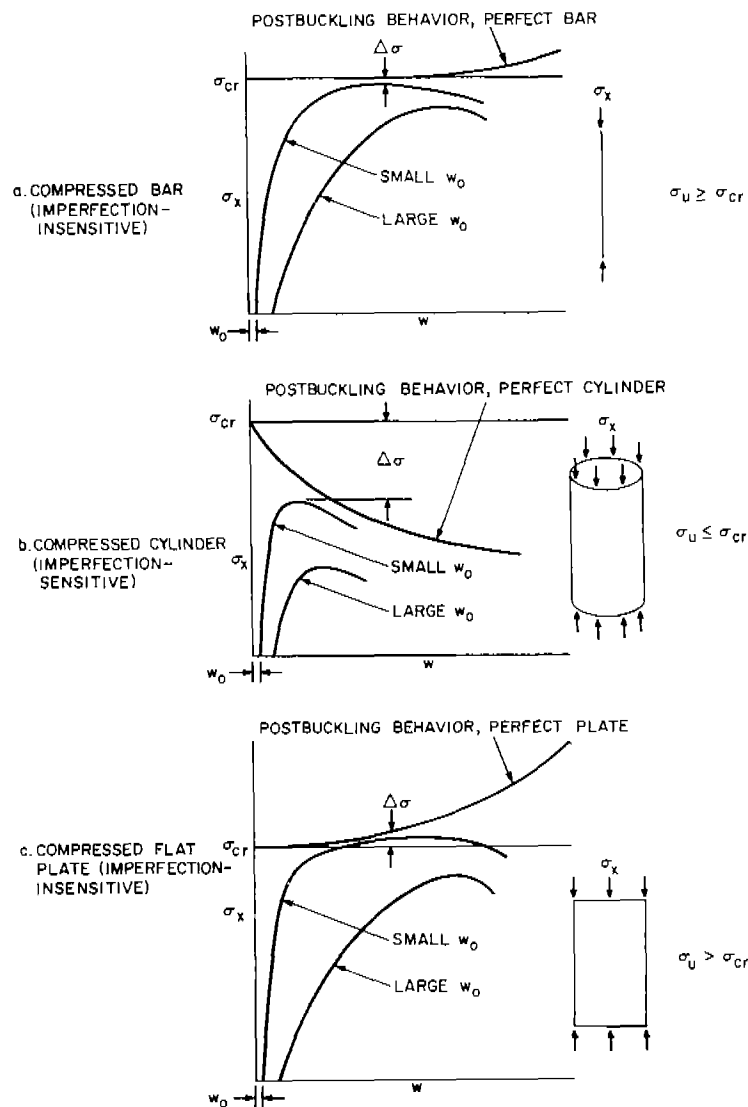


Fig. 8 Effect of Unfairness for Three Types of Structures.

presence of an initial imperfection, w_0 . The effect of unfairness on buckling is large for a compressed cylinder, small for a compressed bar, and negligible (or possibly nonexistent) for a compressed flat plate.

As can be seen in Figure 8c, the failure load of a compressed flat plate can exceed the theoretical buckling load. In the other two cases, that would be improbable for any unfairness, no matter how small.

Important features of the effect of unfairness are the absolute magnitude of the deviation, and the shape and size relative to a buckle mode form. In an imperfection-sensitive structure (Figure 8b), an unfair region of approximately the size and shape of a buckle could induce a loss of 50 percent of the theoretical buckling load if the magnitude of initial unfairness, w_0/t , is of the order 1/10 to 1/2 the thickness. (Values of $w_0/t = 1$ are not uncommon.) On the other hand, if the same cylinder were to be stiffened by bars with a depth equal to 4 or 5 shell thicknesses, there would be essentially no loss of buckling stress from the theoretical value for the stiffened shell. Data on compression buckling of unstiffened shells appear in Appendix II, Figure A2.

Size Effects

It has been well established that there are no size effects in structural behavior where stability is the mode of failure (Ref. 1, 7, 11). The factor which tends to degrade stability behavior (imperfections, or unfairness) is related to nondimensional ratios (r/t and w_0/t , for example). The only consistently significant size effect occurs in material strength properties as a function of plate thickness, grain size, surface phenomena, dislocation density, heat treatment variations, etc. However, these properties appear to exert little influence on stability parameters (Young's modulus, secant and tangent moduli, and Poisson's ratio).

The influence of size may be felt in a practical manner through the degree of unfairness built into ship plating before and during fabrication as result of as-received unfairness and residual stresses induced by welding. These factors could be minimized in the research laboratory where fundamental behavior is being sought.

If proper attention is not paid to unfairness in the laboratory by intentionally including initially imperfect tests in models, then a "size effect" might appear to arise in the prototype. This situation could be circumvented to a large extent by including tests on unfair structures in the laboratory to evaluate the influence of buckling and strength. The most effective method for establishing the reliability of such data is to follow laboratory testing with larger scale models fabricated by methods representative of shipyard construction, measuring the degree of initial unfairness, identifying the magnitude of the proper nondimensional parameter, and then determining whether the strength of that model agrees with theory for the same nondimensionalized degree of unfairness.

Ultimate Compression Strength of Flat Plating

Current Status of Data

Typical design data used by the Navy for computing the strength of flat plating appear in Figure 9, which shows

$$\sigma_u / \sigma_{cy} = 2.25F - 1.25F^2 \quad (13)$$

where

$$F = (t/b) (E/\sigma_{cy})^{1/2}$$

Vasta displayed Eq. (13) as an empirical fit to experimental data on buckling and collapse of a variety of ship steels and one aluminum alloy (Ref. 7). The results appeared in Ref. 8 by Frankland, who referred to Vasta's unpublished data. Vasta also referred to Eq. (13) in discussing large scale testing of ships (Ref. 10).

The experiments of Ref. 7 were conducted on individual rectangular flat plates with the edges under mechanical restraint designed to provide simple support. Tests on other alloys were discussed by Gerard (Ref. 11) and by DTMB (Refs. 12, 13 and 14). The total of those data appear in Figure 10, together with Eq. (13) to reveal the nature of the fit. As may be seen, there is a small but definite difference between the steel data and the results for other materials in the elastic range, but good agreement near σ_{cy} . This difference may affect Figure 9, which includes curves for aluminum alloy plates derived from Eq. (12).

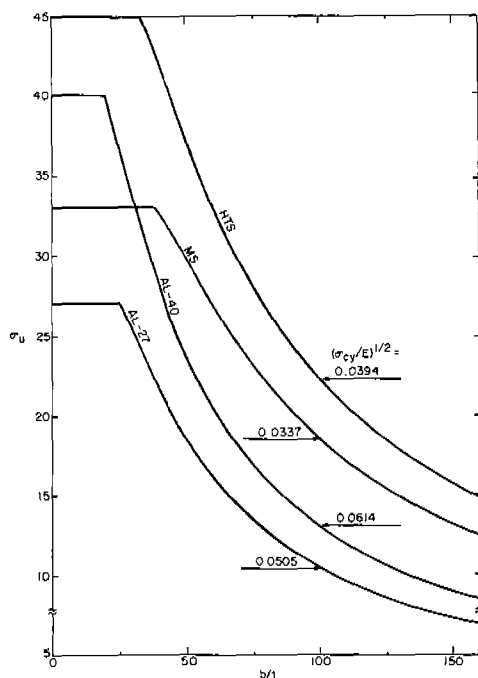


Fig. 9 Ultimate Strength of Uniaxially Compressed Plates ($a/b > 1$).

Tests by Collier on 3-bay panels showed the same behavior as for single plates (Ref. 14). However massive stiffeners were required to force the plates to maximum load. Apparently they maintained simple support along the stiffener lines.

Derivation of Basic Theory

Figure 10 also contains several crosses which refer to a two-flange approach. During this project a preliminary estimate was made into the possibility of developing a fundamental theory of ultimate strength of plates (Appendix I). Existing literature does not appear to include such an approach. In order to derive the theory it was assumed that a buckled plate would continue to support load at $\sigma = \sigma_{cr}$, while load-carrying increases would be confined to the effective strips of plate, b_e , at the edges in accordance with the suggestion of Bengston (Ref. 15). These strips were assumed to act as hinged flanges buckling at a stress level near yield, but taking account of the proper plasticity reduction factor for a hinged flange. The resultant expression was found to be

$$\sigma_u / \sigma_{cy} = 0.11 + 1.77 b_e / b + 0.89 (1 - 2b_e / b) (\sigma_{cr} / \sigma_{cy}) \quad (14)$$

For several selected values of F the corresponding values of σ_u / σ_{cy} from Eq. 14 are shown as crosses in Figure 10. On the basis of the agreement shown, it appears possible to develop a fundamental theoretical approach to achieving an engineering method for determining plate strength.

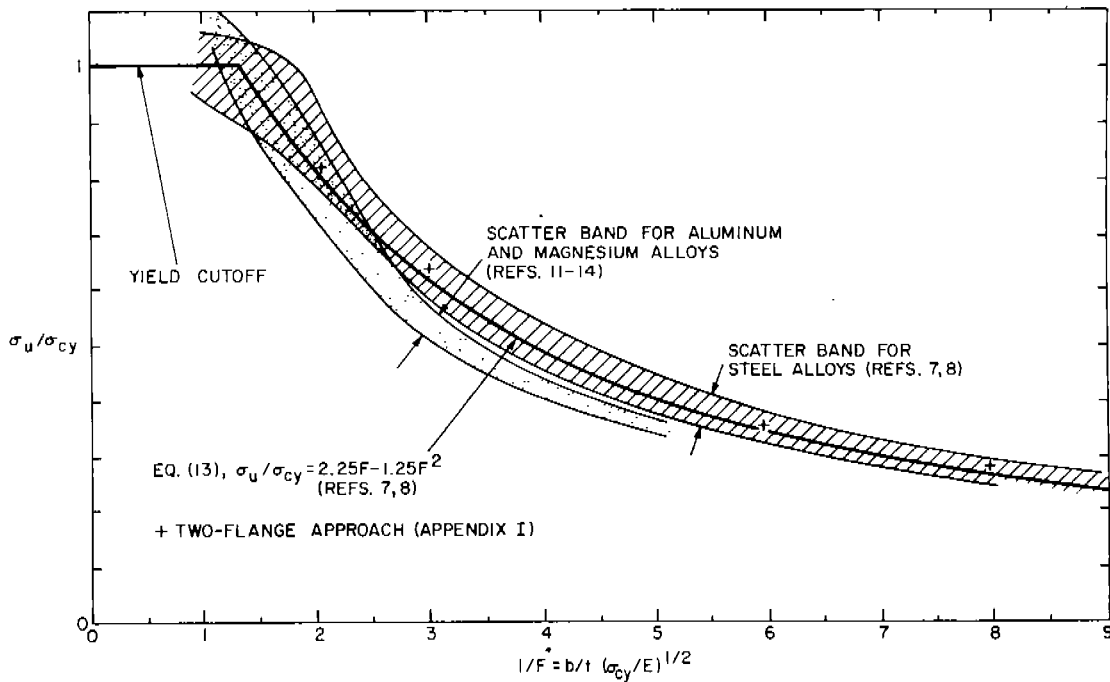


Fig. 10 Theory Compared to Experiment for Ultimate Compression Strength of Simply Supported Flat Plates Without Lateral Pressure Action.

Plate Buckling Under Compression and Normal Pressure

Uniaxial Compression Plus Normal Pressure

Levy, Goldenberg and Zibritosky analyzed theoretically the problem of determining the effect of normal pressure on the buckling stress of a flat plate loaded in uniaxial compression (Ref. 16). For a plate with $a/b = 4$ they obtained the numerical data shown in Table 2.

An alternate approach, recently developed, is described in detail in Appendix II. The basis is the application of shell buckling theory to pressurized plate buckling. Predictions from the new theory also appear in Table 2. Excellent agreement is seen at moderate pressures. The potential advantages of the use of shell theory are as follows:

- 1) Shell theory yields good agreement with theory of Levy et al.
- 2) The shell concept provides a physical picture of the effect.
- 3) As a result of items 1) and 2), the way appears clear to develop reliable design procedures.
- 4) The shell concept leads directly to use of extensive literature from which data can be found on isotropic and orthotropic, elastic and inelastic, shells of single and double curvature.

Table 2. Theoretical Effect of Normal Pressure on Uniaxial Compression Buckling of Flat Plates with $a/b = 4$, $\alpha = (p/E) (b/t)^4$

1. Simple Support		
a	Ref. 16 Theory ¹ σ/σ_{cr}	Shell Theory ¹ σ/σ_{cr}
0	1.00	1.00
2.40	1.06	1.06
12.02	2.24	2.30
24.03	3.09	4.60
2. Clamped		
a	Ref. 16 Theory ¹ σ/σ_{cr}	Shell Theory ¹ σ/σ_{cr}
0	1.00	1.00
15.02	1.06	1.08
37.55	1.30	1.58
¹ As stated in Appendix II, σ and σ_{cr} are the buckling stresses for the pressurized and unpressurized plates, respectively		

- 5) From the extensive background of the manner in which theory and experiment correlate for shell behavior, it is possible to predict whether a reduction could be expected below flat plate buckling for a given case. Furthermore, the amount of reduction can be anticipated, and the use of shell theory would have to be tempered appropriately.

- 6) Because of extensive data on combined loadings for shells, these now could be utilized to predict buckling in the presence of normal pressure (utilizing the shell concept) for such combinations as longitudinal and lateral bending in conjunction with torsion.
- 7) The shell theory predictions of structural behavior can be computerized both for analysis of specific cases, and as part of computerized design of naval vessels.
- 8) The shell concept provides the foundation for understanding the structural behavior of hull bottoms. As a result, although the theory is not perfect in its present form and needs further development, nevertheless it can begin immediately to provide a guide for designing box girder test projects. It offers the potential of achieving significant data by starting with small models of relatively simple geometry in order to check the theory.

The most important feature of the shell theory is the fact that it accounts for initial imperfections, to which axially compressed cylinders are particularly sensitive. As an example, consider a steel plate with $b = 15$ in., $t = 1/4$ in., and $p = 13$ psi. Then the corresponding data would be (Figure A2).

$$\begin{aligned} r/t &= (0.88 \times 3 \times 10^7 / 13) (1/60)^2 \\ &= 560 \\ C &= 0.22 (U = 0.00025, \text{ avg. line}) \\ &= (p/E) (b/t)^4 \\ &= (13/3) 10^{-7} (60)^4 \\ &= 5.6 \end{aligned}$$

In the transition zone, for a simply supported plate (Appendix II)

$$\begin{aligned} \sigma/\sigma_{cr} &= 1 + 0.0272 (\alpha C)^2 \\ &= 1 + 0.0272 (5.6 \times 0.22)^2 \\ &= 1.04 \end{aligned}$$

Through interpolation of the data of Ref. 16, which pertains to plates with no imperfections, σ/σ_{cr} is found to be of the order of 1.6 for the same value of α . This is considerably greater than the value of 1.04, which accounts for initial imperfections as shown in Figure A2.

There are other aspects of the shell theory which cannot be elicited from the approach of Ref. 16. When a cylinder buckles under axial compression, buckling and collapse are simultaneous. Therefore, if an increase in plate buckling could be achieved as a result of the action of the normal pressure tending to shape the plate to a cylindrical surface,

there may be little or no increase in the ultimate strength of the plating. Also the presence of initial unfairness would tend to degrade the magnitude of C for large r/t (small b/t or low p). Three curves for C are presented in Figure A2. They correspond to high quality fabrication for U = 0.00015, moderate quality (or average unfairness) for U = 0.00035. The buckling coefficient decreases as the effect of unfairness becomes increasingly pronounced for a given r/t.

Biaxial Compression Buckling

Timoshenko has shown (Ref. 17) that buckling will occur in a simply supported flat plate under biaxial compression when

$$m^2 \sigma_x + (sa/b)^2 \sigma_y = \sigma_o (m^2 b/a + s^2 a/b)^2 \quad (15)$$

where

$$\sigma_o = \pi^2 D/b^2 t.$$

When σ_x acts alone and $a/b = 1$ or any integer, then $s = a/mb = 1$ and $\sigma_{x_u} = 4\sigma_o$. When σ_y acts alone under the same conditions, $\sigma_{y_{cr}} = \sigma_o$. Using $k_x = \sigma_x/\sigma_o$, $k_y = \sigma_y/\sigma_o$, buckling will occur when

$$k_x + (sa/mb)^2 k_y = (mb/a + sa/mb)^2 \quad (16)$$

A general interaction relation is

$$R_x + R_y = 1 \quad (17)$$

where it is assumed that $n = 1$ in all cases, and

$$R_x = (\sigma_x/\sigma_o) (a/mb + mb/a)^{-2} \quad (18)$$

$$R_y = (\sigma_y/\sigma_o) \left[1 + (mb/a)^2 \right]^{-2} \quad (19)$$

Biaxial Compression Plus Normal Pressure

There is no information in the literature on either buckling or collapse of flat plates or stiffened panels which are loaded by biaxial compression and normal pressure. There is a possibility of utilizing shell buckling theory for this case in the same manner as was described in Appendix II for uniaxial loading. However, it probably would be more complicated because of the difficulty of determining the prebuckling deformation pattern since transverse membrane force would tend to increase the curvature initiated by the lateral pressure.

This aspect of the hull bottom structural behavior would be a more complicated problem for stiffened panels than for flat plates. It might be possible to employ orthotropic theory if the longitudinals were

closer than at present. This is an area in which investigations should begin during the early stages of a test program.

Compression Buckling and Collapse of Stiffened Plating

Introduction

As was indicated above, panel buckling is synonymous with collapse. This places the burden on the stiffeners to support the plating until achievement of the ultimate strength computed from data such as in Figure 10. Because of the additional factors involved, evolution of a technique for analyzing the strength of stiffened panels is more difficult than for plating alone. A few tests were conducted on ship steel panels. However, the aircraft industry acquired the greater mass of experimental data on panels subjected to axial compression alone. Effects of transverse membrane forces, normal pressure and residual stresses are considered in subsequent sections.

Axial Compression Data

Gerard conducted an extensive semi-empirical synthesis of data on panel strength (Ref. 18). Some results appear in Figure 11. A

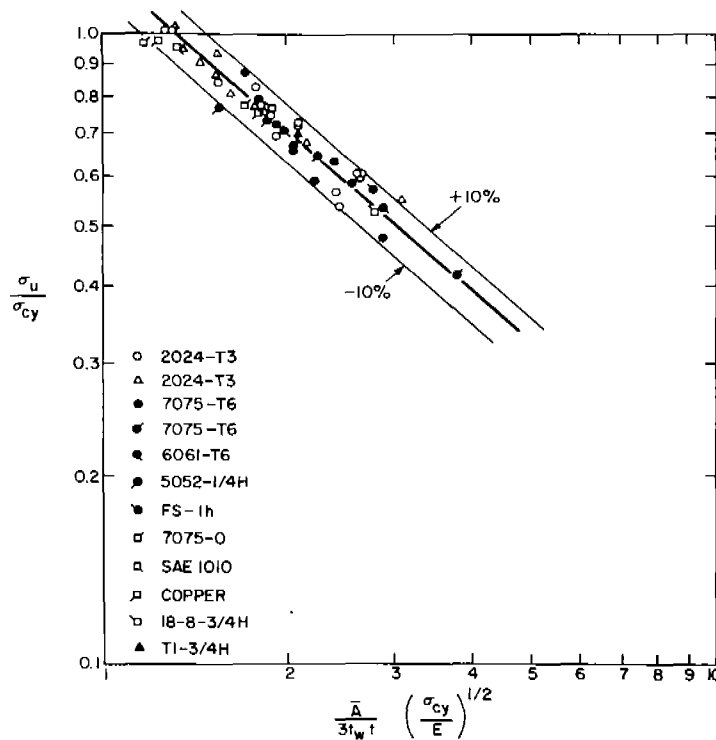


Fig. 11 Crippling Data for 2-Stiffened Panels (Ref. 18.)

large amount of data on different materials are seen to be reducible to relatively few parameters. These can be combined in nondimensional groups to provide a correlation scheme with relatively small scatter. The application of those results to ship construction, however, must be approached with caution since the aircraft data embrace possible failure modes not likely in ship construction. These include buckling of the outstanding legs of stiffeners (flanges), and also stiffener webs. The ultimate load carrying capability of such an element is termed crippling.

Vasta tested stiffened plates to failure and demonstrated the need for sturdy stiffeners to attain σ_u (Ref. 19). Those results are utilized in Part II to assist in designing some of the test specimens.

Axial Compression Plus Normal Pressure

McPherson, Levy and Zibritosky performed compression tests on aluminum alloy panels in combined axial compression and normal pressure (Ref. 20). They found that, with free unloaded edges,

$$\sigma_u / \sigma_{col} = 1 - 0.39 pwa^3 / EI \quad (20)$$

which, in essence, reflects the addition of axial compression and transverse bending stresses.

Lehigh University conducted tests on stiffened panels loaded by normal pressure and performed extensive theoretical analyses to develop design charts. Lee and Ostapenko reported four tests designed to reveal the effect of normal pressure (Ref. 21), with the results shown in Table 3.

Table 3. Summary of Tests on 3 Stiffened Panels Loaded by Axial Compression and Normal Pressure (Ref. 21)

Specimen	Ult. Stress (P/A) (ksi)	Failure Mode	Theoretical Plate Buckling Stress ksi	Lateral Pressure, psi	Mc/I, ksi (computed)	Total, P/A + Mc/I, ksi (computed)
T-1	30.0	Plate Instability	30.0	0	0	30.0
T-2	25.3	Plate Instability	30.0	6.5	3.8	29.1
T-3	22.5	Plate Instability	30.0	13	7.6	30.1
T-4	26.7	Plate Instability	30.0	6.5	3.8	30.5

The effect of normal pressure was small since α was only about 6 at $p = 13$ psi. Theoretically there would have been only a few percent increase in plate buckling stress from that effect.

It is difficult to assess the value of those tests since plate buckling was the failure mode in all cases. Furthermore, as shown in the last column in which the total plating stress was computed from $P/\bar{A} + Mc/I$, the average of T-2, T-3 and T-4 in that column is 29.9 ksi against a theoretical value (and the experimental value for T-1) of 30.0 ksi.

Ostapenko and Lee reported 10 tests in all. The theoretical elastic Euler load for each was much larger than σ_{cy} , which indicated that the strength of each should have been closer to σ_u , which was 33 ksi. However, in no case did the panel achieve this result. Furthermore, only two panels were reported to have failed in column instability. The stronger (T-5) attained a stress level (P/\bar{A}) of 32 ksi with 6.5 psi lateral pressure acting. In both column failure cases, however, the stiffener spacing was considerably less than in the four cases in Table 3. The value of b/t was 40, which corresponds to $(b/t)(\sigma_{cy}/E)^{1/2} = 1.45$ and consequently σ_{cr}/σ_{cy} (and also σ_u/σ_{cy}) should have been approximately 0.9 according to Figure 10. As a result, $\sigma_{cr} = 36$ ksi. For T-5, $Mc/I = 3.3$ ksi, and $P/\bar{A} + Mc/I = 35.3$ ksi. Consequently, a question is raised concerning the reported mode of failure.

If the data of Ref. 21 actually define the trend correctly, then the implication is clear that the longitudinal compression strength of a stiffened panel is reduced by normal pressure directly by the amount of bending stress induced in the cross section at the plating centerline, or

$$P_u/\bar{A} = \sigma_u - Mc/I \quad (21)$$

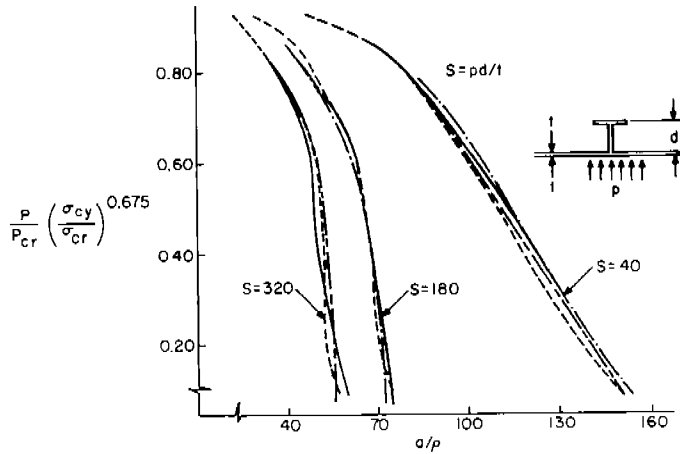
Based on theoretical efforts in consonance with Lehigh test data, Kondo constructed design charts for stiffened plating loaded in axial compression and normal pressure (Ref. 22). One such chart is reproduced in Figure 12a. For large lateral pressure, prediction of the failure load is difficult because of the steepness of the curves. Furthermore, as is shown in Figure 12b, it is possible to synthesize the data by multiplying a/ρ by $S^2/5$. This also has the effect of reducing the curve steepness somewhat.

Grillage Strength

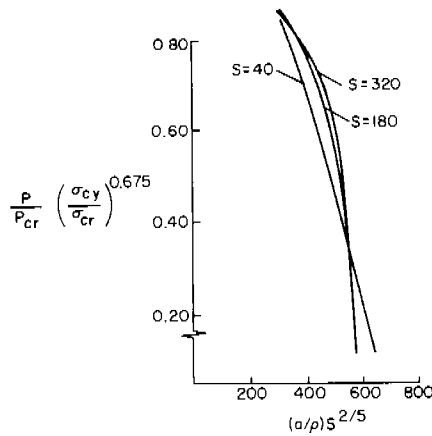
The preceding discussions have concentrated on stiffened and unstiffened plates. However, the problem of hull girder failure involves the interaction of bulkheads, transverse frames, longitudinal stiffeners and plates as a multiple-bay grillage. No data could be found to reveal the strength of a grillage in which the plate has buckled under longitudinal compression. The added influences of normal pressure and transverse compression complicate the problem further since they could tend to degrade the general instability of the grillage in a manner analogous to that in which panel strength may be degraded. Both theory and experiment are required to resolve this problem.

Optimum Design

The possibility of optimizing the design of a structural bay de-



a. Modified Ultimate Strength Curves for Various b/t - Fixed Ends (Ref. 22)



b. Synthesis Using $S^{2/5}$ as Normalizing Factor

Fig. 12 Panel Design Synthesis.

depends upon freedom of choice of the cross section details of the longitudinally stiffened plating, and of transverse rib spacing and geometric characteristics, in order to satisfy the postulate that all instability modes occur simultaneously, as used by Gerard (Ref. 23) and many others. In a ship this freedom is generally not available. As a result non-optimum designs result.

Within this limitation, however, it may be possible to consider arrangement of the longitudinal stiffeners such that the buckling of the plating between stiffeners occurs simultaneously with stiffener webs, flanges, and Euler column action of the panels between the ribs. It may be of value to test such a design in order to establish a reference for weight minimization of future ship designs which could take advantage of optimization because of increased σ_{cy} .

EXPERIMENTAL MECHANICS

Requirements

For the hull girder experiments, it would be necessary to measure accurately the residual and applied stress distributions throughout the model. The applied stresses should be measured before, during and after buckling, in the elastic and inelastic regions of the stress-strain curve of the model material. Deflections would have to be measured to obtain data on effective stiffness of the box, and to probe the model to predict the anticipated buckling and collapse loads.

Available Techniques in Experimental Mechanics (EM)

Numerous EM techniques exist, some in more general use than others, but all with potential usefulness to the hull girder study. Table 4 summarizes the current status of these techniques. The list is ar-

Table 4. Summary of Techniques in Experimental Mechanics

Technique	Principal Value	Yrs. in Use	Flexibility	Limitations	Cost	Time
Bonded Electric Strain Gages	Reveals strain at a point with high precision.	25	HIGH	Not reliable on sheet stock 0.020 in. thick	\$50-500 per installed gage and channel	1-24 hr
Photoelastic Coatings	Reveals strain over a large area.	5	MED.	Reliable only in regions of mild stress gradients on sheets 0.040 in. thick	\$50-100 per installable sheet	1-24 hr
Moire	Reveals strain over a large area.	3	LOW	In the stage of development	Moderate	Moderate
Dial Gages	Reveals deflections at a point with good precision.	50	MED.	Does not reveal strain directly. Analysis required.	Low	Short
Holography	Reveals deflection at a point with good precision.	1	LOW	Long setup and calibration time	High	Moderate

ranged in generally decreasing order of probable utility to the model project. Ranges are seen to be wide for some items (cost to install a strain gage, for example), and data are nonexistent for others.

On the following pages an outline is presented of the attributes and deficiencies of electric strain gages. This is the EM technique which appears to be the prime candidate for use on the hull girder box

beam model project. Principal emphasis is placed on applicability rather than on details of the technical aspects.

Bonded Electric Strain Gages

Attributes

1. High reliability and accuracy of results when installed and read by properly trained personnel.
2. Strains as large as 5 per cent may be sensed using certain types of gages.
3. Data are obtainable at concentrations in large structures.
4. Mean membrane normal and shear strains, and bending and twisting strains, may be recorded in plates. Principal strain magnitudes and directions are derivable from those results.

Deficiencies

1. Gage can be used only in a selected small region. Acquisition of strain distribution data may require numerous gages, which must be applied in pairs on opposite sides of a plate. Furthermore, if principal directions are not known beforehand, a minimum of three gages per side (or a total of 6) is required to provide complete data reliably at a single point. If high accuracy is required to large inelastic strains, then two different types of gages are needed; i. e., one for precise data at small strains and one for large strains. This, then, requires 12 gages at a selected station. Also, they cannot be applied at exactly the same location. Consequently, the set is useful only where strain gradients are not severe.
2. The presence of the strain gage on a thin metal plate (less than 0.020 in. thick) interferes with the accuracy of the information it is supposed to provide by stiffening the plate locally.
3. Current gages for large strain sensing are about 1 inch long, which limits application to regions of small strain gradient.
4. A bonded electric strain gage may not be removed and re-applied. Therefore, if a gage station is lost as a result of model damage, the set of gages at that station must be replaced when the repair is completed.
5. For maximum accuracy and reliability, a pair of shielded lead wires from each gage, and appropriate temperature compensating gages, are required to complete the electric circuitry to the bridge readout. Consequently, it would not be feasible to move the model in order to alter the manner of loading. Therefore, extensive planning of data logistics

and experimental procedures may be required for conducting tests on a large scale model.

OPTIMUM EXPERIMENTAL PROGRAM

The optimum program for the hull girder project is defined as that combination of models, loading systems, data acquisition methods and theoretical analysis which would provide satisfactory correlation of theory and experiment at minimum cost, with minimum time as a subsidiary consideration.

One of the many possible approaches embraces extensive use of experimental mechanics followed by plotting of the data according to more-or-less arbitrary parameters in the hope of eventually achieving a correlation scheme for constructing a unified empirical design chart such as Figure 10. In that case, attainment of a clear understanding of mechanisms would be minimized, if not entirely absent.

An alternate approach might center on an active search for a theory derived from fundamental considerations, with current data (Figure 10 and Appendix I, for example) as a guide. These could be followed by relatively few tests on models fabricated to a small scale to obtain a check on the theory and to help establish the numerical values of parameters such as n in Appendix I.

It is the purpose of this section to examine rationally the factors which are involved in achieving the optimum project and to compare types of projects on the basis of satisfactory correlation of theory and experiment.

MATERIAL SELECTION

The purpose of the intended test project would be to reveal possible modifications to the basic design chart (Figure 2) which might result from the effects of normal pressure and lateral membrane forces. As is seen in Figure 10, there is scatter in the failure data for a magnesium alloy, several aluminum alloys and a few steels. However, when it is considered that several investigators provided the data, the agreement is reasonably good. Furthermore, the effects of plasticity may account for a large part of the difference between the ferrous and the nonferrous alloy data.

This situation with regard to longitudinal compression data, and the discussion on modeling laws, indicate the possibility of conducting the box girder tests on only one model material without prejudicing the generality of the results for other materials. Changes in Figure 10 due to lateral pressure and transverse membrane compression might apply equally to several ship-building materials in the b/t range in which elastic buckling would occur since only σ_{cy} and E appear to be involved. In the inelastic buckling range the effects of the shape of the stress-strain curve might be of minor consequence since the stress levels would approach the yield cutoff.

For the sake of obtaining a few check points, there may be value in conducting a few small-model studies on materials other than the chosen model material, for which hot rolled steel looms as the prime

candidate, as would appear in Table 5 below. However, a decision in this regard need not be made until the primary goals of the intended box girder project will have been satisfied. At that time, factors such as time and funding can be weighed in arriving at that decision.

The method of manufacture should be the simplest possible, which dictates use of a material which would be available (before forming) to a high degree of flatness and which could be used to construct test articles with maximum ease. These features dictate the use of hot rolled steel sheet, which was used in many of the examples in the section on Model Design. The properties appear in Table 5. It was one of the materials used to achieve the correlation shown in Figure 10 for uniaxially compressed plates.

Table 5. Comparison of Model Materials

Material	σ_{cy} ksi	E Msi	SHAPING		JOINING			Repairing
			Machining	Forming	Welding	Brazing	Soldering	
Cold Rolled Steel	60	30	good	fair	good	good	good	fair
Hot Rolled Steel (furniture steel)	35	29	good	good	good	good	good	fair
6063-T5 Aluminum	21	10	fair	good	good	poor	poor	fair
Cartridge Brass	25	13	excellent	good	good	good	good	good
10% Phosphor Bronze	100	15.9	good	good	good	good	good	good
Beryllium Copper	110	18.5	good	good	good	good	good	good
Hysol Epoxy	8	0.48	fair	no	no	no	no	good
Plexiglass	8	0.5	good	no	no	no	no	good

MODEL FABRICATION

Shape Generation

Small models can be fabricated with little effort from flat, rectangular plates joined at the edges to form boxes, angles, Tees and a variety of structural shapes. In hot rolled steel the joining process can be performed by soldering or brazing without introducing significant residuals or causing unfairness. Such procedures can be used for brass sheet also, but they cannot be performed on structural aluminum alloys.

One of the more recent developments in manufacturing technology is the use of electron beams to weld metallic structures. The technique is applicable to a variety of materials, among which are steels, and the various alloys of aluminum, magnesium, titanium and beryllium.

Attributes of the process are a narrow heat-affected weld zone, minimum distortion of the welded structure, and negligibly small residual stresses. Complex details such as Tee-stiffened plates can be fabricated with relative ease. The use of the technique is particularly recommended for such structures if they are fabricated to a small size. This could be a problem for use of brazing or more conventional welding of the small models contemplated for the proposed test project for evaluation of hull girder strength, especially in the construction of single bay and continuous grillages.

Demonstration box models of 0.016 in. thick furniture steel were tested in compression and yielded results that agreed well with Figure 10. Despite excessive model distortion after collapse, the electron-beam-welded edges of those models remained joined, which indicates the soundness and strength of the connection. This would be an important factor in achieving reliability in the test program.

In the manufacture of small models (for photoelastic studies, as an example) components have been shaped to close tolerances, after which they were joined with the aid of jiggling fixtures which were simple to construct and which involved moderate cost. The same techniques could be utilized in any contemplated test project to study plate strength using small models.

Upon completion of the models, strain gages could be installed at appropriate locations. It is also possible to install strain gages on model components before joining. This would permit acquisition of data from otherwise inaccessible locations.

On a model to be tested in compression, the final operation would involve careful grinding of the loading edges to insure flatness and parallelism.

Multiple Tests on a Model

The economy of the test project can be increased if the number of tests on a given model is large. This would require some means of repairing a model after failure testing, which in turn imposes a design requirement to include sufficient flexibility in the model to permit repairs.

An alternate possibility is the use of a technique such as NDTs described in Appendix IV, the purpose of which is to conduct tests at loads below instability levels. By proper probing procedures at $\sigma \ll \sigma_{cr}$ it is theoretically possible to identify instability loads. Details have been discussed in Appendix IV, in which some cases of structural shapes and loads are considered. Further study of the procedure is required before it is universally applicable. Yet, it may provide a useful adjunct to the anticipated test project through achievement of a balance with the multiple-testing requirement.

Sealing

Because of the requirements to apply internal vacuum to some of the models, means must be provided for sealing the structure against leakage. This can be accomplished by using thick loading plates which could be joined to the model ends (for compression testing) by cement or solder. It also would be possible to use undercut plates with O-rings in the grooves. However, such details could be decided during the test program. In any event, the larger the model the more difficult the sealing problem.

MODEL DESIGN

Introduction

For purposes of discussion, the region of prime concern may be chosen as the typical structural bay shown in Figure 1. It has been depicted as a regular rectangular array, for simplicity.

The problem area of interest is a plate of length a , width b , and thickness t , simply supported ($w = 0$) along all four edges up to buckling, and hopefully to collapse. The loads are N_x , N_y and p_z . They are assumed to be uniform on and within the plate boundaries.

It is a purpose of this project to identify ranges of dimensions and magnitudes of loads for test articles so as to achieve realistic representations of ship proportions in general, with emphasis on the strengths of plates panels and grillages. For these purposes, such features as intermediate decks need not be duplicated. Stiffener proportions and sizes would be identified to permit plates to achieve the strength attainable as single plates in strong supporting fixtures. The basic data for model design appear in this section.

Modeling Laws for Plates

N_x Alone

As shown in Figure 10, both buckling and strength of uniaxially compressed plates may be related to σ_{cy} , E and b/t with apparently little need for additional parameters, if a modest scatter band is acceptable. Although there are numerical differences in the relationships, the basic character may be expressed in the nondimensional form

$$\sigma_{cr}/\sigma_{cy} = 2.25F - 1.25F^2 \quad (13)$$

where

$$F = (t/b) (E/\sigma_{cy})^{1/2}$$

For model studies of the uniaxial compression strength of a simply supported rectangular plate, the five pertinent quantities for the model would be the same as for the prototype, no matter what the proportions and material of the prototype, or the proportions and

material of the model. Furthermore, b_m , t_m , E_m , and σ_{cy_m} need not be matched (or even in proportion) with the same prototype quantities as long as

$$\left[(b/t) (E/\sigma_{cy}) \right]_m^{1/2} = \left[(b/t) (E/\sigma_{cy}) \right]_p^{1/2} \quad (22)$$

in order to ensure that

$$\left(\sigma_u / \sigma_{cy} \right)_m = \left(\sigma_u / \sigma_{cy} \right)_p \quad (23)$$

Therefore, although Eq. (13) is empirical, Eqs. (22) and (23) provide an acceptable modeling law for uniaxially compressed rectangular plates with simply supported edges. Some additional support may be found in the theoretical derivation shown in Appendix I, which yields the same form as Eq. (13) for the expression for plate strength.

$$N_x, N_y \text{ and } p_z$$

There is no known relationship for the strength of rectangular flat plates under combinations of N_x , N_y and p_z . Consequently, it is necessary to develop both a theory and experimental data for these cases. During the course of this project an initial exploration of such a possibility was begun by attempting to expand the result of Appendix I. However, it was evident that the problem was too complex to permit completion during the performance period of this project. This cursory study did indicate, however, that Eqs. (22) and (23) could be used as the core of a modeling law provided that the effects of N_y and p_z could be included properly. For an initial step, the plotting of experimental data should be conducted as on Figure 10, after which synthesis of the data could be conducted. At the same time, the theoretical development of Appendix I should be expanded to include the influence of N_y and p_z .

Model Scaling Laws

Throughout this report it is assumed that the model represents properly the structural behavior of the prototype. That is to say, they satisfy the right scaling law. Eqs. (22) and (23) are pertinent to uniaxially compressed plates, for example. If the model and prototype are fabricated from the same material, then the modeling law reveals that buckling will occur at the same stress level for each, and the same will apply to failure.

If the materials differ, then

$$\sigma_{cr_m} / \sigma_{cr_p} = \sigma_{u_m} / \sigma_{u_p} = \sigma_{cy_m} / \sigma_{cy_p} \quad (24)$$

Consequently proper scaling would be achieved by altering every prototype dimension by the same multiplier. In addition, if

$$(\sigma_{cy}/E)_m \neq (\sigma_{cy}/E)_p \tag{25}$$

then

$$(b/t)_m \neq (b/t)_p \tag{26}$$

Table 6 depicts the corresponding range of b/t for models fabricated from a variety of materials, when compared to $20 \leq (b/t)_p \leq 80$ for HY-80 steel.

Table 6. Ranges of $(b/t)_m$ for Various Materials with $20 \leq (b/t)_p \leq 80$

Material	σ_{cy} (ksi)	E (Msi)	$(\sigma_{cy}/E)^{1/2}$	Range of $(b/t)_m$
HY-80	80	30	0.0516	20.0 to 80
Hot Rolled Steel	35	29	0.0347	29.7 to 119
6063-T5 Aluminum Alloy	21	10	0.0448	23.1 to 92
Brass	25	13	0.0439	23.5 to 94

In order to guide the testing program toward realism in the model, the AOE-2 was used as a reference throughout this project. For that vessel $L = 770$ ft. It is assumed that $\sigma_{cy} = 35$ ksi and $E =$ Msi, corresponding to hot rolled steel. At the midship section $b = 30$ in. and maximum $t = 1.25$ in. The corresponding data for models of that ship to various scales, made from different materials, appear in Table 7.

Table 7. Plate Widths and Thicknesses for AOE-2 Models to Various Scales, Steel vs. Aluminum

Material	Model Length and Scale Factor							
	L = 770 ft.		L = 193 ft.		L = 77 ft.		L = 15.4 ft.	
	$\Sigma = 1$		$\Sigma = 1/4$		$\Sigma = 1/10$		$\Sigma = 1/50$	
	b in.	t in.	b in.	t in.	b in.	t in.	b in.	t in.
Hot Rolled Steel (Furniture Steel)	30.0	1.25	7.50	0.313	3.00	0.125	0.60	0.025
6063-T5 Aluminum Alloy	30.0	1.61	7.50	0.404	3.00	0.161	0.60	0.0323

At 1/50 scale the plate thickness approaches the usable minimum for reliable data with strain gages as the experimental technique. It also is important to recognize the possible need for controlling the scale of a model in order to employ a standard gage. In the cases in Table 7, 0.025 and 0.032 both are near standard, with some allowance for thickness. They are slightly thinner than Ref. 19 gages.

The proportions of the AOE-2 represent a significant departure from previous naval vessels in that the cross section area of the longitudinal stiffening system is 35 percent of the plate section, and a/b is of the order of 1 instead of 2 to 4 while b/t is low at 24 as contrasted to the hitherto more common range from 40 to 60. If b/t is chosen at 60 and b = 30 in. (as possibly representative of other surface vessels) than the data in Table 7 are modified to the values shown in Table 8.

Table 8. Plate Widths and Thicknesses for Models Corresponding to $b_p = 30$ in. and $t_p = 1/2$ in. Various Scales, Steel vs. Aluminum

Material	Model Length and Scale Factor							
	L = 500 ft.		L = 125 ft.		L = 50 ft.		L = 25 ft.	
	$\Sigma = 1$		$\Sigma = 1/4$		$\Sigma = 1/10$		$\Sigma = 1/20$	
	b in.	t in.	b in.	t in.	b in.	t in.	b in.	t in.
Hot Rolled Steel (Furniture Steel)	30.0	0.500	7.50	0.125	3.00	0.050	1.50	0.025
6063-T5 Aluminum Alloy	30.0	0.646	7.50	0.161	3.00	0.0646	1.50	0.0323

The minimum thickness is achieved with 1/20 scale.

Effect of Scale

The total cost of a test project depends upon a number of factors. Broad considerations such as the location of the test (industrial, government or university laboratory) could influence costs of fabrication, instrumentation, test conduct, data acquisition, reduction and analysis. The type of capital equipment on hand also could be a factor in some cases.

Model size has been chosen here as the basic independent variable for comparison of programs. The cost of model fabrication would be a large fraction of the test project. It could account for 1/3 to 1/2 of the total. It is often possible to estimate fabrication costs on the basis of dollar per pound of completed article. This would lead to a cubic cost scaling law

$$\$m = \$p(L_m/L_p)^3 = \$p\Sigma^3 \quad (27)$$

where L_p actually refers to some selected reference test article.

However, if welding is the principal means of fabrication, then plate thickness and length would control and a parabolic cost scaling law might result

$$\$_m = \$_p (L_m/L_p)^2 = \$_p \Sigma^2 \quad (28)$$

Some indication of the predictions provided by Eq.(28) may be obtained from the fact that certain stiffened aluminum alloy models about 1 foot long cost \$100 to \$200 to build, with almost all the cost absorbed by labor. On that basis the AOE-2 structure would cost between 60 and 120 million dollars to build, while a box girder 40 feet long would cost 160,000 to 300,000 dollars using Eq. (28). These figures do not account for complexities of structural details. On the other hand they indicate the sensitivity of testing costs to model scale and emphasize the value of minimizing model size.

Model Loadings

Longitudinal Compression, N_x

The longitudinal force per inch of lateral width, N_x , can be computed from

$$N_x = t\sigma_x \quad (= t\sigma_u \text{ at failure}) \quad (29)$$

for a typical plate in the structural grillage. When the longitudinal stiffener area, A_s , is included in an effective thickness $\bar{t} = t + A_s/b$, then

$$N_x = \bar{t}\sigma_x \quad (= \bar{t}\sigma_u \text{ at failure}) \quad (30)$$

In the past, A_s/b has been of the order of $t/10$. In the AOE-2 the ratio is 0.35, or approximately $1/3$.

On the basis of selected values of b/t for hot rolled steel and several prototype plate widths, it is possible to identify longitudinal loadings on various scale model panels, as shown in Table 9. These are used to aid in the establishment of the model test structural details presented schematically in the following section. They employ the data in Figure 10.

Transverse Compression, N_y

The ratio N_y/N_x would vary from near zero for a long shallow ship with several full-width intermediate decks, to the order of 1 for a relatively short deep ship comprised of a simple box. Therefore, the selection of specific test values for N_y could be accomplished by arbitrarily selecting several values of N_y/N_x within the extremes, 0 and 1, with the assurance that the structural behavior of virtually any ship could be encompassed within that range.

Table 9. Ranges of Ultimate N_x (kip/in) for Hot Rolled Steel Plates

RANGES OF ULTIMATE N_x (KIP/IN) FOR HOT ROLLED STEEL PLATES

	b/t								
	20			50			80		
(b/t) $(\sigma_{cy}/E)^{1/2}$	0.694			1.735			2.776		
σ_u (ksi)	35.0 (Cutoff)			30.8			22.8		
t (in)	0.025	0.050	0.200	0.025	0.050	0.200	0.025	0.050	0.200
b (in)	0.500	1.00	4.00	1.25	2.50	10.0	2.00	4.00	16.0
N_x (kip/in)									
$A_s/bt = 0$	0.88	1.75	7.00	0.77	1.54	6.16	0.51	1.14	4.50
1/10	0.96	1.92	7.70	0.85	1.69	6.76	0.63	1.25	5.02
1/3	1.17	2.33	9.33	1.03	2.07	8.25	0.76	1.52	6.08

Vertical Pressure, p_z

The maximum bottom pressure, p_z , would be equivalent to the waterlevel elevation plus the wave height which would be associated with the longitudinal strength design bending moment. If that total height were to be 60 ft., for example, then p_z would be $0.44 \times 60 = 26.4$ psi.

Vertical pressure on the model would be the same as on the prototype if $\sigma_m = \sigma_p$ with $p_z = 0$. The pressure is scaled only to stress, not to model size.

MODEL LOADING SYSTEMS

Types of N_x Loading Systems

The forces on a box model could be applied by internal vacuum in combination with either transverse bending or axial compression to generate N_x , N_y and p_z on a test bay. The uniformity of loading would be maintained to σ_{cr} in the plate. At higher loading levels in a bending test there would be a shift in the neutral axis of the beam and elementary bending theory no longer would yield σ_x in the test bay. Experimental mechanics would be required to identify stress distributions.

No neutral axis shift would occur in the case of the axially compressed box. Load redistribution would occur in that case also when $\sigma_x > \sigma_{cr}$. However, compression tests could prove the simplest method of loading to provide all the necessary data for the project.

The simplicity of box loading would be lost in panel tests for which complex jiggling and bagging would be required to induce N_x , N_y and p_z . However, there would be no need to measure test bay loads other than through the load applicators themselves. On the other hand,

as soon as plate buckling initiated, it still would be necessary to measure plate and stiffener loads for forces in the postbuckling range.

Load Applicators

Forces may be applied to small or moderate-size models through suitable jiggling in a universal testing machine. Individual force applicators are available in a variety of forms such as hydraulic jacks, cables with calibrated dynamometers, and dead weights, to name a few. The latter grouping would be used in larger scale testing in conjunction with appropriate structural floors or frames.

Types of p_z and N_y Loading Systems

The simplest method for applying transverse pressure to a plate or panel would be through internal evacuation of a box structure, which could be effected efficiently to pressure as high as 13 psi. This would not induce a sufficiently large magnitude of N_y however. Auxiliary devices would have to be employed for that purpose, which could be accomplished by transverse load applicators. These may be found in small portable testing machines. Devices also may be constructed with little effort using hydraulic jacks, as has been done for a variety of specialized tests in many experimental laboratories.

CONCLUSIONS

1. Prediction of ultimate strength of uniaxially compressed metal plates can be made with good reliability using the empirical relation

$$\sigma_u / \sigma_{cy} = 2.25 F - 1.25 F^2$$

where $F = (t/b) (E/\sigma_{cy})^{1/2}$

2. Development of a reliable fundamental plate ultimate strength theory for uniaxial loading appears feasible.
3. Transverse membrane stresses can reduce significantly the longitudinal buckling load for a rectangular plate. The degradation is a function of the plate aspect ratio, a/b .
4. Normal pressure may increase critical N_x for a rectangular plate. The effect would be largest for large a/b .
5. Initial imperfections and residual stresses may degrade the critical N_x for a rectangular plate.
6. No data exist for prediction of ultimate strength of plates under a combination of N_x , N_y and p .

7. The buckling stress of a plate in a panel under N_x and p_z appears to be essentially the same as under N_x alone. The only effect of the normal pressure apparently is to reduce N_x so that the combined axial load and bending stresses equal the plate uniaxial buckling stress.
8. When a/B is small and a/b is large, a panel would behave essentially as a column in which case free unloaded edges would be an appropriate test method.
9. Proper representation of hull structural features may be accomplished with simple models provided that the emphasis is upon evaluation of plate strength as distinguished from panel strength.
10. Data are required to evaluate the strength of structural grillages, and to assess the influence of continuity across bulkheads and the effectiveness of deep transverse frames in providing support to the panels.
11. The most efficient method of experimental mechanics for determination of plate stresses to high precision is bonded electric strain gages.
12. An effective low cost hull girder strength testing project appears feasible using small models made from hot rolled steel typical of metal furniture construction. Through extensive research the technical reliability of small scale model testing has been well established.

RECOMMENDATIONS

Initial Project

In order to establish a base for predicting hull girder strength, the following initial effort is recommended:

- a. All tests should be conducted on small models using plates of the order of 0.025 in. thick.
- b. Fabricate models from hot rolled steel sheets, which are usually flat and have a well-defined compression yield.
- c. Conduct tests on unreinforced boxes, and on boxes with longitudinally reinforced plates.
- d. Use $a/b = 3$ for all models.
- e. Use bonded electric strain gages to obtain structural data to aid in identification of buckling and failure.
- f. Perform tests under N_x , N_x and p_z , N_x and N_y , and finally combined N_x , N_y and p_z . Maximum $N_y/N_x = 1$ and maximum internal $p_z = -13$ psi.
- g. Select 3 values of b/t to cover the range of behavior which might be anticipated in ship construction.

- h. Test a 3-bay box grillage with longitudinal stiffeners and intermediate deep transverse frames to assess the influence of end restraint and transverse support on the panels.
- i. Conduct investigations to establish a fundamental theory to correlate with the results of the test project.

Test Details

Two types of boxes are considered appropriate to the initial goals of the intended test project as outlined in the Recommendations. They are a square cross section box without stiffening, and a rectangular section box with stiffening on opposite walls (Figure 13). The primary loading N_x , should be induced by axial compression. Pressurization could be accomplished by internal evacuation, and N_y could be applied by a transversely oriented load applicator such as a portable testing machine.

The models should be fabricated from hot rolled steel sheet by soldering or brazing to minimize possible modification of the mechanical

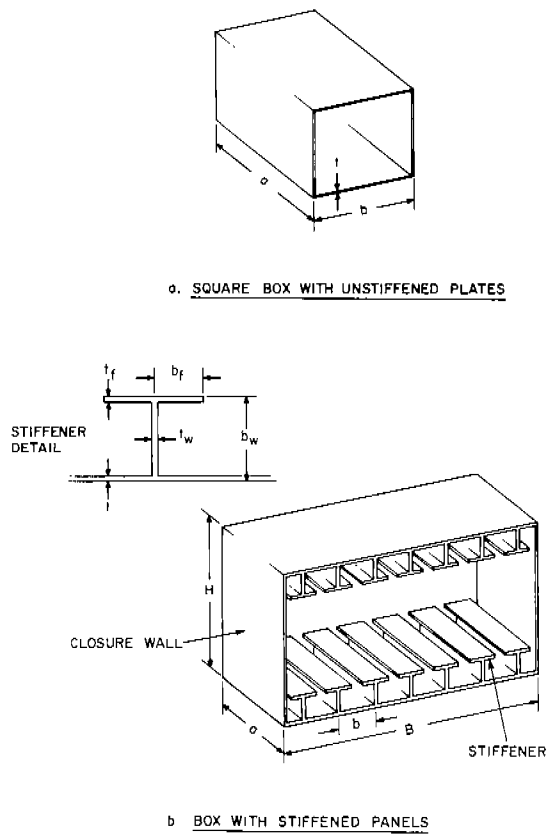


Fig. 13 Two Types of Test Boxes.

properties of the material. Compression stress-strain curves should be determined as a part of the test program.

Simple Boxes

The nominal sheet thickness of 0.025 in. used above for comparison studies actually is an average between 0.0239 in. and 0.0269 in., two gages in which furniture steel usually is available. Either may be selected for minimum size models. If the thicker is used, then the box data would be as shown in Table 10. The minimum value of b/t has been increased to 30, which would provide a better datum than the previously chosen value of 20 in the preceding examples.

Table 10. Details of Minimum Size Unstiffened Furniture Steel Boxes, with $t = 0.0269$ in., $a/b = 3$

		b, in.	a, in.	σ_u , ksi	N_{x_u} lb/in.	P_u /plate, lb
	30	0.807	2.421	35.0	942	760
b/t	50	1.345	4.035	30.8	829	1,120
	80	2.152	6.456	22.8	611	1,320

Stiffened-Plate Boxes

In order to minimize the possible influence of boundary constraints, the panel width should be large relative to the length. This can be accomplished by using the same a , b and t values as shown above, with 7 longitudinals on each of the stiffened panels. Then, with 8 plate widths per panel, $B = 8b = 5.656$ in., 10.76 in. and 17.22 in., corresponding to $b/t = 30$, 50 and 80 respectively. The lengths would be the same as shown above.

The preliminary design of the Tee stiffeners should be based on the data shown in Ref. 19. Using $t_f = t_w$, $b_f/t_f = 10$, and $b_w/t_w = 20$, the data appear in Table 11.

Table 11. Tee Stiffener Dimensions and Panel Loads for 3 Minimum Size Test Panels. See Figure 13 for Symbols. The thicknesses are standard gages, and $a/b = 3$

	t_w , in.	t_f in.	b_w in.	b_f in.	A_s in.	A_s/bt	N_{x_u} kip/in.	B, in.	P_u /panel kip	
	30	0.0269	0.0269	0.538	0.269	0.0289	1.33	2.19	6.456	14.1
b/t	50	0.0269	0.0269	0.538	0.269	0.0289	0.80	1.49	10.76	16.0
	80	0.0418	0.0418	0.836	0.418	0.0694	1.21	1.35	17.22	23.1.

The first two designs ($b/t = 30$, 50) are based on use of the minimum gage, 0.0269 in.

Effects of Transverse Framing

The preceding sections of these recommendations have been focused on determination of plate strength, with and without longitudinal stiffening. The final problems to be considered are the effect of transverse frames on the strength of the hull girder between bulkheads, and the influence of grillage continuity across bulkheads. To provide test data on these problems it would be desirable to simulate these effects in tests on panels for which the strength will have been determined previously.

The theory pertaining to this case would be based upon extension of general instability theory for a grillage by taking into account the influence of early buckling of the plates. Initial steps could be taken into the development of the theory. However, it is realistic to expect that extensive treatment (as well as extensive testing of multiple-bay grillages, if necessary) should be relegated to a later phase of the test project.

The data can be obtained by performing transverse bending tests (combined with N_y and p_z) on a box of length $9a$, with bulkheads at $3a$ and $6a$, and with deep transverse frames at a , $2a$, $4a$, $5a$, $7a$ and $8a$. Tests could be performed on this multiple bay model with $b/t = 50$. On a multiple span beam the carryover of structural behavior from the outer bays to the middle bay would vary little from a 3-bay beam to a 5-bay beam. Therefore, since failure would probably occur in the center bay of a multiple-bay grillage, the choice of a 3-bay box was made for economy and ease of model construction.

By use of appropriate constraints in the model, data could also be obtained for the single-bay box depicted in Table 9.

The deep transverse frames for the 3 bay box could be Tee-shaped in cross-section. They could be fabricated with $t_w = t_f = 0.0418$ in., $b_w = 0.836$ in. and $b_f = 0.418$ in. These dimensions were obtained by proportioning data from various sources (Ref. 18 among them) and after examination of the AOE-2 structure.

Six types of box models would then be tested in compression in this initial project: 3 unstiffened single-bay boxes, 2 longitudinally stiffened single-bay boxes, and 1 three-bay box with longitudinal stiffeners and transverse deep frames. The load combinations were discussed previously. The continuous grillage tests would be performed in transverse loading to induce longitudinal bending.

Subsequent Projects

When reliable strength prediction procedures for unstiffened and stiffened plates and continuous grillages have been established from the preceding effort, the investigations should be extended to evaluate the following effects both theoretically and experimentally in order to broaden the range of useful application of the procedure:

- a. Choice of material (HY-80, aluminum alloy, and others)
- b. Plate aspect ratio, a/b

- c. Unfairness and residual stresses
- d. Nonuniformity of applied stress distribution
- e. Internal structural details
- f. High normal pressure (up to 25 psi, and possibly more)

Additional plate strength problem areas include

- a. Shear (N_{xy})
- b. Shear together with N_x , N_y , and p_z in various combinations
- c. Stiffener design for panel strength under the preceding load combinations.

ACKNOWLEDGMENTS

The contributions of Messrs. John Pozerycki and Angelo Colao during the course of the project and the preparation of this report are gratefully acknowledged.

REFERENCES

- 1) Gerard, G., and H. Becker, "Handbook of Structural Stability-Parts I-VII," NACA TN 3781-6, and NASA TN D-162, 1957-8.
- 2) Cooper, P. B., "Literature Survey on Longitudinally Stiffened Plates," Lehigh University. Fritz Eng. Lab. Report 304-2, Sept. 1963.
- 3) Bryan, G.H. "On the Instability of a Plate Under Thrusts in Its Own Plane with Application on the Buckling of the Sides of a Ship", Proc. London Mathematical Society, v. 22, 1891, p. 54ff.
- 4) Stowell, E. Z., "Compressive Strength of Flanges", NACA TR 1029, 1951.
- 5) Gerard, G., "Secant Modulus Method for Determining Plate Instability Above the Proportional Limit", Jour. Aero. Sci., v. 13, no. 1, Jan. 1946, pp. 38-44, 48.
- 6) Gerard, G., and S. Wildhorn, "A Study of Poisson's Ratio in the Yield Region," NACA TN 2561, Jan. 1952.
- 7) Vasta, J., Unpublished U. S. Experimental Model Basin Progress Reports.

- 8) Frankland, J.A., "The Strength of Ship Plating Under Edge Compression," U. S. Experimental Model Basin Report 469, 1940.
- 9) Rampetsreiter, R.H., T. T. Lee and A. Ostapenko, "Tests on Longitudinally Stiffened Flat Panels," Lehigh University Fritz Eng. Lab. Report 248. 5, 1962.
- 10) Vasta, J., "Lessons Learned from Full Scale Ship Structural Tests," Trans. SNAME, v. 66, 1958.
- 11) Gerard, G., "Handbook of Structural Stability, Part IV Failure of Plates and Composite Elements," NACA TN 3784, Aug. 1957.
- 12) Duffy, D. J., and R. B. Allnutt, "Buckling and Ultimate Strengths of Plating Loaded in Edge Compression. Prog. Rep. No. 1, 6061-T6 Alum. Plates." DTMB Report 1419, Apr. 1960.
- 13) Conley, W. F., L. A. Becker and R. B. Allnutt, "Buckling and Ultimate Strength of Plating Loaded in Edge Compression. Prog. Rep. No. 2-Unstiffened Panels". DTMB Report 1682, May 1963.
- 14) Collier, J. S., "Ultimate Strength of Plating Loaded in Edge Compression Effect of Adjacent Panels." NSRDC Report, Apr. 1967.
- 15) Bengston, H. W., "Ship Plating Under Compression and Hydrostatic Pressure". Trans. SNAME, V. 47, no. 80, 1939, pp. 80-116.
- 16) Levy S., D. Goldenberg and G. Zibritosky, "Simply Supported Long Rectangular Plates Under Combined Axial Load and Normal Pressure", NACA TN 949, Oct. 1944.
- 17) Timoshenko, S., "Theory of Elastic Stability", McGraw-Hill, 1936.
- 18) Gerard, G., "Handbook of Structural Stability, Part V-Compressive Strength of Flat Stiffened Panels, "NACA TN 3785, Aug. 1957.
- 19) Vasta, J., "Compression Tests of Ship Structure Assemblies." U. S. Exp. Model Basin Report 452, June 1938.
- 20) McPherson, A.E., S. Levy and G. Zibritosky, "Effects of Normal Pressure or Strength of Axially Loaded Sheet-Stringer Panels," NACA TN 1041, July 1946.
- 21) Lee, T. T., and A. Ostapenko, "Tests on Longitudinally Stiffened Plate Panels Subjected to Lateral and Axial Loading", Lehigh University, Fritz Eng. Lab. Report 284. 4, 1960.
- 22) Kondo, J., "Ultimate Strength of Longitudinally Stiffened Plate Panels Subjected to Combined Axial and Lateral Loading," Lehigh University, Fritz Eng. Lab. Report 284, 13, 1965.
- 23) Gerard, G., "Minimum Weight Analysis of Compression Structures," New York University Press (Interscience); 1956.

24) "Some Investigations of the General Instability of Stiffened Metal Cylinders, III-Continuation of Tests of Wire-Braced Specimens and Preliminary Tests of Sheet-Covered Specimens," Guggenheim Aeronautical Laboratory, California Institute of Technology, NACA TN-907.

APPENDIX I

ULTIMATE STRENGTH OF PLATES

Theory

It is the purpose of this Appendix to demonstrate the possibility of developing a basic theory for predicting the ultimate stability strength of flat plates subjected to various loadings by using the case of uniaxial compression as an example. The approach was developed from a modification of a suggestion by Bengston (Ref. 15) regarding the assumption of load distribution.

The force balance, referring to Figure A1, is based on the hypothesis that the plate centerline stress is σ_{cr} at all load levels equal to, or greater than, the buckling load. Then

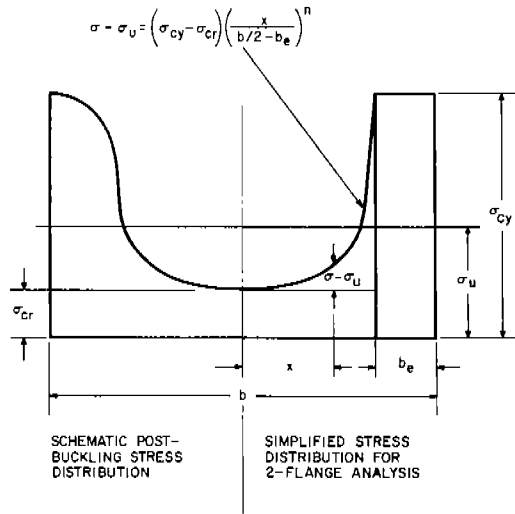


Fig. A1 Assumed Stress Distribution for Two-Flange Analysis.

$$b\sigma_u = 2b_e\sigma_{cy} + (b-2b_e)\sigma_{cr} + 2(\sigma_{cy}-\sigma_{cr}) \int_0^{b/2-b_e} \left(\frac{x}{b/2-b_e}\right)^n dx \quad (A1)$$

Since the last term becomes

$$(\sigma_{cy}-\sigma_{cr})(b-2b_e) / (n+1) \quad (A2)$$

then

$$b\sigma_u = 2b_e\sigma_{cy} + (b-2b_e) \left(\frac{n}{n+1} \sigma_{cr} + \frac{1}{n+1} \sigma_{cy} \right) \quad (A3)$$

$$= 2b_e \left(\frac{n}{n+1} \right) \sigma_{cy} + \left(\frac{b}{n+1} \right) \sigma_{cy} + (b-2b_e) \left(\frac{n}{n+1} \right) \sigma_{cr}$$

or

$$\sigma_u / \sigma_{cy} = 2(b_e/b) \left(\frac{n}{n+1} \right) + \left(\frac{1}{n+1} \right) + \left(\frac{n}{n+1} \right) (1-2b_e/b) \frac{\sigma_{cr}}{\sigma_{cy}} \quad (A4)$$

Each edge strip may be considered a hinged flange which buckles at σ_{cy} , with consideration given to the effect of plasticity, so that

$$\sigma_{cy} = \frac{0.433 \pi^2 E}{12(1-\nu_e^2)} \left(\frac{t}{b_e} \right)^2 \frac{E_s}{E} \frac{1-\nu_e^2}{1-\nu^2} \quad (A5)$$

where 0.433 is the buckling coefficient for the flange. Then

$$b_e/b = (CF)^{1/2} \quad (A6)$$

where

$$C = \left[\frac{0.433 \pi^2}{12(1-\nu_e^2)} \right]^{1/2} = 0.626 \text{ with } \nu_e = 0.3 \quad (A7)$$

$$F = (t/b)(E/\sigma_{cy})^{1/2} \quad (A8)$$

$$\eta = \frac{E_s}{E} \frac{1-\nu_e^2}{1-\nu^2} \quad (A9)$$

The plasticity reduction factor may be approximated by the relation

$$\eta = (1 + 0.002E/\sigma_{cy})^{-1} \quad (A10)$$

Results

Several numerical values of σ_u/σ_{cy} were computed for $\sigma_{cy} = 33$ ksi, $E = 10$ Msi, $n = 8$ (for a sharp rise in the $\sigma - \sigma_u$ curve), and with consideration given to the effect of plasticity in computing σ_{cr} , Eq. (2). The result is the relation

$$\sigma_u / \sigma_{cy} = 0.11 + 1.77b_e/b + 0.89(1 - 2b_e/b) (\sigma_{cr}/\sigma_{cy}) \quad (A11)$$

which is shown as crosses on Figure 10. They agree well with the empirical curve.

APPENDIX II

SHELL THEORY FOR PLATE BUCKLING UNDER PRESSURE

Introduction

When a flat plate is subjected to normal pressure the out-of-plane deflections cause curvature in two directions. When $a/b \gg 1$, the deflected shape approaches a segment of a cylinder. The edges are assumed to be supported laterally only ($w = 0$). No membrane forces are considered to act along the edges. If longitudinal compression is applied to the deflected plate then the resultant instability may be computed from cylinder shell theory for certain proportions of the plate and for certain ranges of normal pressure.

This Appendix summarizes the present results of studies that are being conducted on this new approach to determination of plate buckling under N_x and p .

Summary of Current Results

The three classes of behavior are the flat plate, transition or short cylinder, and moderate length cylinder. In the flat plate range

$$\sigma/\sigma_{cr} = 1 \tag{A12}$$

where the elastic plate buckling stress is

$$\sigma_{cr} = \frac{4\pi^2 E}{12(1 - \nu_e)^2} \left(\frac{t}{b}\right)^2 \tag{A13}$$

and σ/σ_{cr} is the ratio of the pressurized plate buckling stress to that of the flat, unpressurized plate.

In the transition and moderate length cylinder regimes the effect of initial imperfections can play an important role. In a perfect cylinder the elastic compressive buckling stress is

$$\sigma_{cr} = \left[3(1 - \nu_e^2) \right]^{-1/2} Et/r \tag{A14}$$

However, extensive experimental data show large departures from that relation as r/t becomes large. A more reliable relation is found to be

$$\sigma_{cr} = CEt/r \tag{A15}$$

with C determined from Figure A2. The three values of U relate to small imperfections ($U = 0.00015$), medium, and large imperfections. By including this effect, it is found that, in the transition range, for simply supported plates, with $\alpha = (p/E) (b/t)^4$,

$$\sigma/\sigma_{cr} = 1 + 0.0272(\alpha C)^2 \quad (A16)$$

or, if $C = 0.6$ (small r/t)

$$\sigma/\sigma_{cr} = 1 + 0.0098\alpha^2 \quad (A17)$$

For clamped plates

$$\sigma/\sigma_{cr} = 1 + 0.0010(\alpha C)^2 \quad (A18)$$

or, if $C = 0.6$ (small r/t)

$$\sigma/\sigma_{cr} = 1 + 0.00036\alpha^2 \quad (A19)$$

In the cylinder range, which applies to plates with large a/b and large α ,

$$\sigma/\sigma_{cr} = 0.3\alpha C \quad (A20)$$

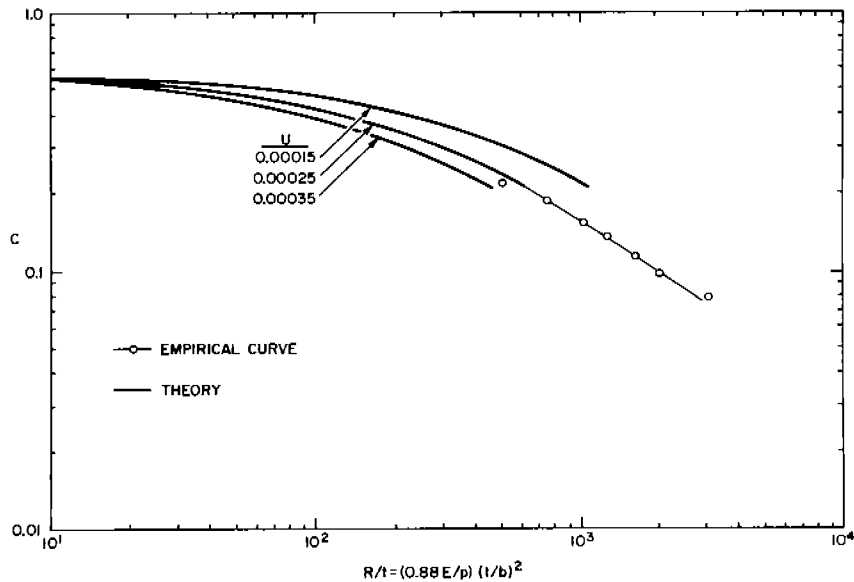


Fig. A2 Modified Classical Buckling Coefficient as a Function of r/t for Axially Compressed Cylinders.

APPENDIX III
BIAXIAL BUCKLING OF FLAT PLATES

The basic relation for biaxial buckling of simply supported flat plates is presented by Timoshenko (Ref. 17)

$$m^2 \sigma_x + (sa/b)^2 \sigma_{cy} = (\pi^2 D/a^2 t) \left[m^2 + (sa/b)^2 \right]^2 \quad (A21)$$

For ship plates, $a/b > 1$ and $s = 1$ as a rule. Also, the buckling stresses usually are computed with respect to the width, b , so that $\pi^2 D/b^2 t$ would be a more desirable grouping than $\pi^2 D/a^2 t$. Then, with $\pi^2 D/b^2 t = \sigma_o$, and $\sigma_x/\sigma_o = k_x$, $\sigma_y/\sigma_o = k_y$

$$k_x + (a/mb)^2 k_y = (a/mb + mb/a)^2 \quad (A22)$$

When $k_y = 0$, Eq. (A22) becomes the unminimized classical relation for a long compressed plate. When $k_x = 0$, Eq. (A22) becomes the classical result for a wide column with $m = 1$ and $a/b \gg 1$.

If both sides are divided by $(a/mb + mb/a)^2$, then

$$R_x + R_y = 1 \quad (A23)$$

where

$$R_x = \frac{k_x}{(a/mb + mb/a)^2} \quad (A24)$$

$$R_y = \frac{k_y}{\left[1 + (mb/a)^2 \right]^2} \quad (A25)$$

When $m = a/b$ (square wave buckling), $R_x = k_x/4$, $R_y = k_y/4$ and

$$k_x + k_y = 4 \quad (A26)$$

If $k_y = rk_x$ to meet a given loading ratio, then for a specific a/b the permissible value of k_x may be found from

$$k_x = \frac{(a/mb + mb/a)^2}{1 + r(a/mb)^2} \quad (A27)$$

in which several integral values of m must be selected to find the lowest k_x .

APPENDIX IV

NONDESTRUCTIVE TESTING FOR STRUCTURAL STABILITY

Basis

When a structure loses strength through instability, the approach to the unstable condition with increasing load is accompanied by a loss of rigidity. The nature of the relation between rigidity loss and magnitude of load level depends upon the type of structure and the type of rigidity being considered or measured.

Approach

The nondestructive procedure for determining the instability load of a structure involves measurement of the rigidity at selected load levels and then extrapolating the data in the proper manner to obtain the magnitude of the load at which rigidity would vanish. The manner of extrapolation would depend upon the structure and the type of rigidity being measured. An example is depicted in Figure A3 which shows how transverse bending stiffness of a column can be used to identify the Euler load. The procedure is essentially that of the "normal restraint coefficient" approach which was explored by GALCIT in the early 1940's (Ref. 24), but which was not exploited because of the lack of agreement of the measured buckling loads with predicted values for aircraft type cylinders subject to bending general instability.

Work at MITHRAS

Recently, studies have been conducted at MITHRAS on the possibility of establishing a general procedure for NDTs. Several cases have been investigated for columns, and an analysis has been made for predicting general instability of a stiffened cylinder which shows agreement with the same GALCIT data that did not correlate with the normal restraint coefficient prediction. The reason for the lack of the GALCIT correlation became clear through these recent investigations.

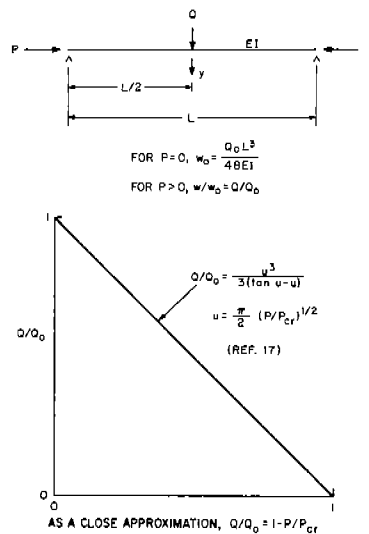


Fig. A3 Behavior of a Centrally Loaded Beam-Column.

Column Behavior

Through the use of mathematical relations presented by Timoshenko (Ref. 17) for the amplification of lateral deflection in a beam which is subjected to axial load, it is a simple matter to portray the manner in which the bending rigidity decays as the axial load is raised. The results for several types of transverse loads appear in Figure A4. It is evident that the lateral load ratio is nearly a linear function of the column load ratio. The deviation can be approximated reasonably well by a sinusoidal curve.

The relation for a central transverse force is linear to within a fraction of a percent. This may be the most important from the standpoint of technical applicability, since it is likely that development of a probing procedure would revolve around this manner of loading.

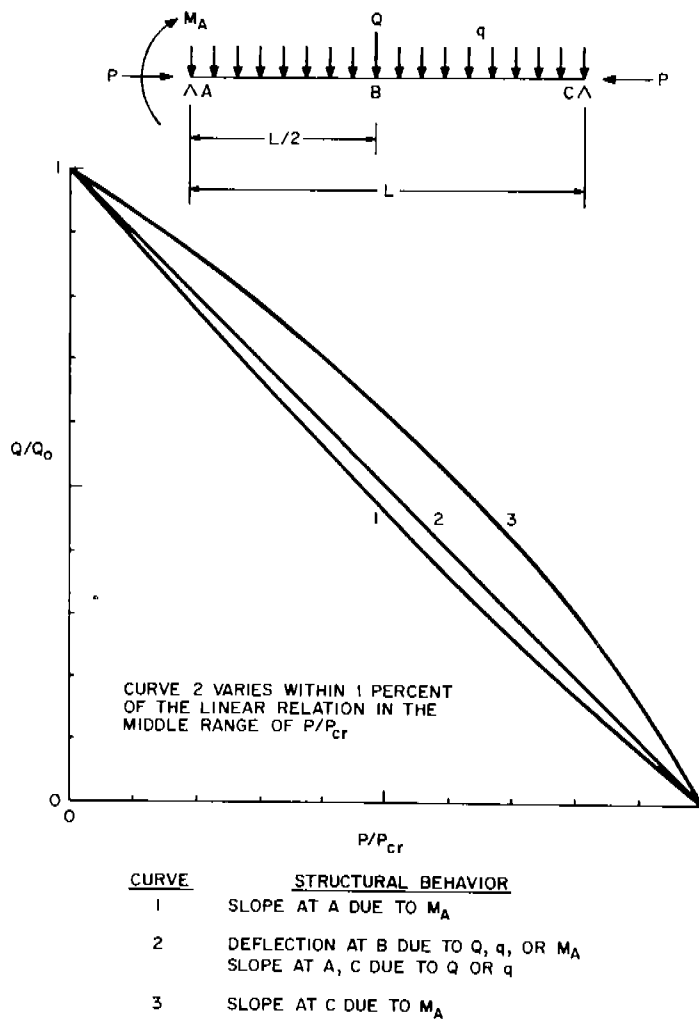


Fig. A4 Behavior of Various Beam Columns.

Cylinder Behavior

A mathematical analysis was conducted for a long isotropic cylinder loaded in axial compression and subjected to a ring of radial inward forces uniformly distributed around the median plane circle (Figure A5). The results indicated that there should be a linear relation between the square of the radial force ratio and the axial load, instead of a linear relation between both ratios as tried by GALCIT. When the parabolic relation was used to predict the instability load for the GALCIT cylinder described in Ref. 24, excellent agreement was obtained with the experimental observation, as shown in Figure A5. In addition, when the parabolic relation between testing force ratio and axial load ratio is plotted from the mean of the scatter band for the squared relation, it is seen to agree well with the GALCIT probe data. Consequently, because the GALCIT probing was discontinued at about 75 percent of instability, the data appeared to fit a linear relation fairly well but to indicate an instability load which was much larger than the measured value.

Current Status

Several cases have shown the possibility of a practical probing method for evaluating instability in a structure without requiring the application of a structural loads which are large proportions of the instability loads. It is important to identify the proper relation between the probe forces and the applied loads for each type of structure. An encouraging result is the agreement of the theoretical probing procedure (for a ring of forces on a long isotropic cylinder in compression) with experimental data (for a single radial force as a probe to determine bending general instability in a stiffened cylinder).

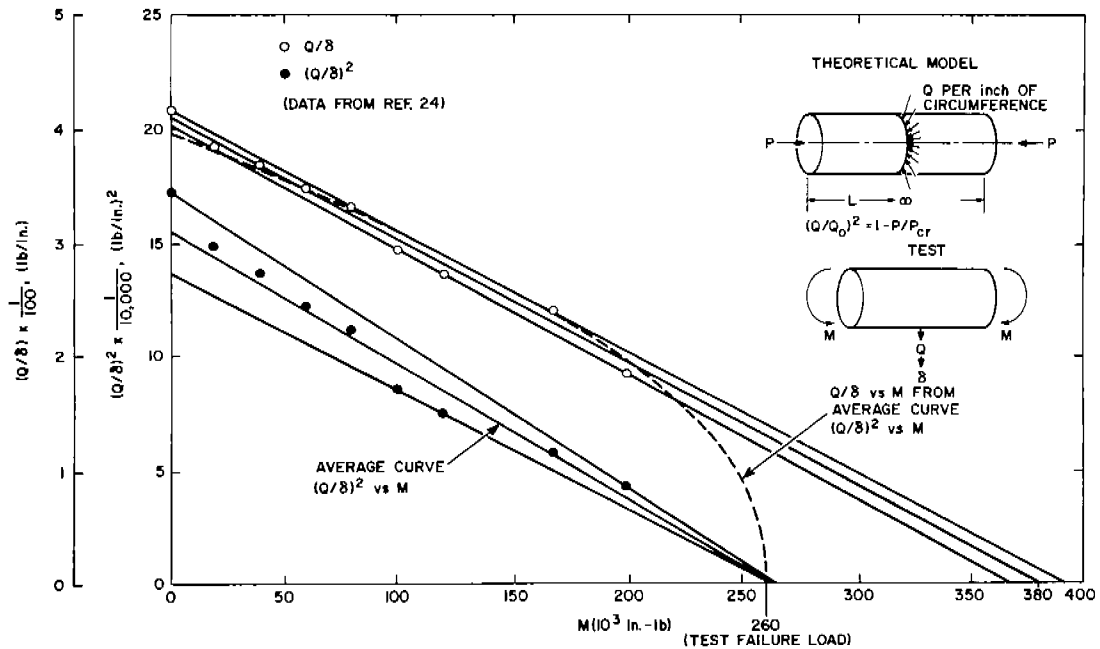


Fig. A5 Bending General Instability of Stiffened Cylinder.

DOCUMENT CONTROL DATA - R & D

(Security classification of title, body of abstract and indexing annotation must be entered when the overall report is classified)

1. ORIGINATING ACTIVITY (Corporate author) MITHRAS, a division of Sanders Associates, Inc. 701 Concord Avenue Cambridge, Mass. 02138		2a. REPORT SECURITY CLASSIFICATION None	
		2b. GROUP	
3. REPORT TITLE FEASIBILITY STUDY OF MODEL TESTS ON SHIP HULL GIRDERS			
4. DESCRIPTIVE NOTES (Type of report and inclusive dates) Final Technical Report (28 June 1968 through 28 September 1968)			
5. AUTHOR(S) (First name, middle initial, last name) Herbert D. Becker			
6. REPORT DATE May 1969		7a. TOTAL NO OF PAGES vii + 50	7b. NO OF PAGES 24
8a. CONTRACT OR GRANT NO. N00024-68-C 5468		9a. ORIGINATOR'S REPORT NUMBER(S) M-7006 R1 (BTX)	
b. PROJECT NO. SF 013-03-04			
c. Task 2022, SR-183		9b. OTHER REPORT NO(S) (Any other numbers that may be assigned this report) SSC-194	
d.			
10. DISTRIBUTION STATEMENT No restrictions			
11. SUPPLEMENTARY NOTES		12. SPONSORING MILITARY ACTIVITY Naval Ship Systems Command Washington, D. C.	
13. ABSTRACT An efficient program is identified for strength testing of hull girder models representative of longitudinally framed ship construction. The purpose of the tests is to generate data (for correlation with theory where available) to provide the basis for engineering design of the primary structure of the hull girder. The major loads are longitudinal compression induced by primary hull bending, normal pressure from the sea, and athwartship compression induced by the horizontal pressure on the sidewalls. The results of the evaluation indicate the feasibility of a project which would begin with a number of compression tests using steel box models less than one foot long. The purpose is to establish basic behavior and to provide inputs to assist in developing a reliable strength theory which would have general utility over a wide range of parameters relevant to hull girder design.			

14.

KEY WORDS

hull girders
stability

LINK A

LINK B

LINK C

ROLE

WT

ROLE

WT.

ROLE

WT

NATIONAL ACADEMY OF SCIENCES-NATIONAL RESEARCH COUNCIL

DIVISION OF ENGINEERING

This project has been conducted under the guidance of Advisory Group II, Ship Research Committee. This is a committee of Maritime Transportation Research Board, National Academy of Sciences-National Research Council. The Committee has cognizance of Ship Structure Committee projects in materials, design and fabrication as relating to improved ship structures. In addition, this committee recommends research objectives and projects; provides liaison and technical guidance to such studies; reviews project reports; and stimulates productive avenues of research.

SHIP RESEARCH COMMITTEE

Chairman: M. L. Sellers, (I, II, III)
Naval Architect
Newport News Shipbuilding and Drydock Co.

Vice Chairman: J. M. Frankland (I, II, III)
(Retired) Mechanics Division
National Bureau of Standards

Members

W. H. Buckley (I, II)
Chief, Structural Criteria
Bell Aerosystems Company

B. B. Burbank (III)
(Retired) Chief Metallurgist
and Chemist
Bath Iron Works Corp.

D. P. Clausing (III)
Senior Scientist
U. S. Steel Corporation

D. P. Courtsal (II, III)
Principal Hull Design Engineer
Dravo Corporation

A. E. Cox (I, II)
LHA Project Director
Newport News Shipbuilding
and Drydock Company

F. V. Daly (III)
Manager of Welding
Newport News Shipbuilding
and Drydock Co.

J. F. Dalzell (I)
Senior Research Scientist
Hydronautics Incorporated

J. E. Goldberg, (I, II)
School of Civil Engineering
Purdue University

J. E. Herz (I, II)
Chief Structural Design Engineer
Sun Shipbuilding and Drydock Co.

G. E. Kampschaefer, Jr. (III)
Manager, Application Engineering
ARMCO Steel Corporation

B. R. Noton (II, III)
Visiting Professor
Dept. of Aeronautics and Astronautics
Stanford University

W. W. Offner
Consulting Engineer

S. T. Rolfe (III), *Coordinator*
Section Supervisor
U. S. Steel Corporation

M. Willis (I) *Coordinator*
Assistant Naval Architect
Sun Shipbuilding and Drydock Co.

R. A. Yagle (II), *Coordinator*
Dept. of Naval Architecture
and Marine Engineering
University of Michigan

(I) - Advisory Group I, *Ship Strain Measurement & Analysis*

(II) - Advisory Group II, *Ship Structural Design*

R. W. Rumke (III) - Advisory Group III, *Metallurgical Studies*

Executive Secretary

SHIP STRUCTURE COMMITTEE PUBLICATIONS

These documents are distributed by the Clearinghouse, Springfield, Va. 22151. These documents have been announced in the Technical Abstract Bulletin (TAB) of the Defense Documentation Center (DDC), Cameron Station, Alexandria, Va. 22314, under the indicated AD numbers.

- SSC-180, *Experimental Determination of Plastic Constraint Ahead of a Sharp Crack under Plane-Strain Conditions* by G. T. Hahn and A. R. Rosenfield. December 1969. AD 646034.
- SSC-181, *Results from Full-Scale Measurements of Midship Bending Stresses on Two Dry-Cargo Ships -- Report #2* by D. J. Fritch, F. C. Bailey, J. W. Wheaton. March 1967. AD 650239.
- SSC-182, *Twenty Years of Research under the Ship Structure Committee* by A. R. Lytle, S. R. Heller, R. Nielsen, Jr., and John Vasta. December 1967. AD 663677.
- SSC-183, *Metallurgical Structure and the Brittle Behavior of Steel* by Morris Cohen. May 1968.
- SSC-184, *Exhaustion of Ductility in Compressed Bars with Holes* by S. Kobayashi, and C. Mylonas. June 1968. AD 670487.
- SSC-185, *Effect of Surface Condition on the Exhaustion of Ductility by Cold or Hot Straining* by J. Dvorak and C. Mylonas. July 1968. AD 672897.
- SSC-186, *Effect of Ship Stiffness upon the Structural Response of a Cargo Ship To An Impulsive Load.* by Manley St. Denis and Samuel N. Fersht. September 1968. AD 675639.
- SSC-187, *Biennial Report of Ship Structure Committee.* September 1968. AD 675022.
- SSC-188, *Effect of Repeated Loads on the Low Temperature Fracture Behavior of Notched and Welded Plates* by W. H. Munse, J. P. Cannon and J. F. Kiefner. October 1968. AD 676722.
- SSC-189, *The Video Tape Recording of Ultrasonic Test Information* by Robert A. Youshaw, Charles H. Dyer and Edward L. Criscuolo. October 1968. AD 677894.
- SSC-190, *Bending Moment Distribution in a Mariner Cargo Ship Model in Regular And Irregular Waves of Extreme Steepness* by Naresh M. Maniar and Edward Numata. November 1968. AD 689187.
- SSC-191, *Plastic Flow in the Locale on Notches and Cracks in Fe-3Si Steel Under Conditions Approaching Plane Strain* by G. T. Hahn and A. R. Rosenfield. November 1968.
- SSC-192, *Notch Brittleness After Fracture* by C. Mylonas and S. Kobayashi. December 1968.
- SSC-193 *Development of Mathematical Models for Describing Ship Structural Response in Waves* by Paul Kaplan. January 1969.